European Journal of Medicinal Chemistry 61 (2013) 132–145

Contents lists available at SciVerse ScienceDirect

European Journal of Medicinal Chemistry

journal homepage: http://www.elsevier.com/locate/ejmech

Original article

Design, synthesis and *in vitro* anti-proliferative activity of 4,6-quinazolinediamines as potent EGFR-TK inhibitors

Samar Mowafy [a], Nahla A. Farag [a], Khaled A.M. Abouzid [b,*]

[a] Pharmaceutical Chemistry Department, Faculty of Pharmacy, Misr International University, Abbassia, 11566 Cairo, Egypt
[b] Pharmaceutical Chemistry Department, Faculty of Pharmacy, Ain Shams University, Abbassia, 11566 Cairo, Egypt

ARTICLE INFO

Article history:
Received 2 February 2012
Received in revised form
24 September 2012
Accepted 11 October 2012
Available online 27 October 2012

Keywords:
4-Anilinoquinazoline
EGFR-TK inhibitors
Docking study
Anti-proliferative activity

ABSTRACT

4-Anilino-6-substituted-quinazolines were designed, synthesized and evaluated for EGFR-TK and tumor growth inhibitory activities. The target compounds were designed with enamine ester or urea moieties appended at the C-6 of quinazoline as additional hydrogen bond acceptor functions. Most of the synthesized compounds displayed potent EGFR-TK inhibitory activity at 10 μM and the 6-ureido-anilinoquinazoline derivative **7a** showed IC_{50} value of 0.061 μM. Moreover, six compounds were tested by National Cancer Institute (NCI), USA for their anti-proliferative activity at 10 μM in full NCI 60 cell panel. Compound **7a** was further assayed for five dose molar ranges in full NCI 60 cell panel and exhibited remarkable growth inhibitory activity pattern against Non-Small Cell Lung Cancer EKVX (GI_{50} = 0.37 μM), NCI-H322M (GI_{50} = 0.36 μM), Renal Cancer A498 (GI_{50} = 0.46 μM), TK-10 (GI_{50} = 0.99 μM) and Breast Cancer MDA-MB-468 (GI_{50} = 1.096 μM) which are of high EGFR expression. Docking study was performed for the active compounds into ATP binding site of EGFR-TK which showed similar binding mode to gefitinib and additional binding with Cys-773 at the gatekeeper of EGFR-TK enzyme.

1. Introduction

The epidermal growth factor receptor (EGFR) protein belongs to the ErbB family of receptor tyrosine kinases (RTKs) which plays an important role in the regulation of cell growth, differentiation, and survival [1]. EGFR is a glycoprotein that contains an extracellular ligand-binding domain, a transmembrane region, and an intracellular domain with kinase activity [2]. EGFR is over expressed in several human tumors including Non-Small Cell Lung Cancer (NSCLC), prostate, breast and ovarian cancers [3–10] and correlates with a poor prognosis in many cancer patients [11]. Thus, EGFR is an attractive target for the design and development of compounds that can specifically bind to the receptor and inhibit its tyrosine kinase (TK) activity and its signal transduction pathway in cancer cells. Inhibition of EGFR has been achieved through two main approaches: by blocking ligand binding to the extracellular domain with monoclonal antibodies and by using small-molecule inhibitors that interact at the ATP-binding site [12]. A well-studied class of these latter inhibitors is represented by 4-anilinoquinazolines, exemplified by the lead compound gefitinib, erlotinib which are approved by the FDA for the treatment of advanced Non-Small Cell Lung Cancer [13], Fig. 1. These agents belong to the 4-anilinoquinazoline class of inhibitors and the key features between the receptor and this template have been revealed as follows [14,15]. (1) The quinazoline core fits into the ATP binding pocket of the kinase domain, where the N-1 nitrogen of the quinazoline nucleus interacts with the backbone NH of Met-769 via a hydrogen bond, and water mediated hydrogen bonding is observed between the N-3 of the quinazoline and the Thr-766 side chain. (2) The aniline ring fills an adjacent lipophilic pocket. (3) The solubilizing side chains at C-6 and/or C-7 of the quinazoline core act to improve physical properties and confer a more favorable pharmacokinetic profile.

In the past decade, the SAR study of quinazoline as EGFR inhibitors was directed toward the modification of the C-4 arylamino group [16], by varying the aniline substitution pattern, fine tuning of the kinase selectivity profile can be achieved [17]. Also, the substitution at C-6 position of quinazoline has received increasing attention in the development of more potent & selective inhibition [9,17]. Almost all substituents in this position were designed to bind with Cys-773 in EGFR through hydrogen bonding or covalent bonding [16,18,19]. Since 6-position of quinazoline points toward the outside of the protein & theoretical studies have indicated that bulky substituents are tolerated at the 6-position. Moreover the 6-position substitution allows optimum distance for

* Corresponding author. Tel.: +20 1222165624; fax: +20 225080728.
E-mail address: Khaled.abouzid@pharm.asu.edu.eg (K.A.M. Abouzid).

0223-5234/$ – see front matter © 2012 Elsevier Masson SAS. All rights reserved.
http://dx.doi.org/10.1016/j.ejmech.2012.10.017

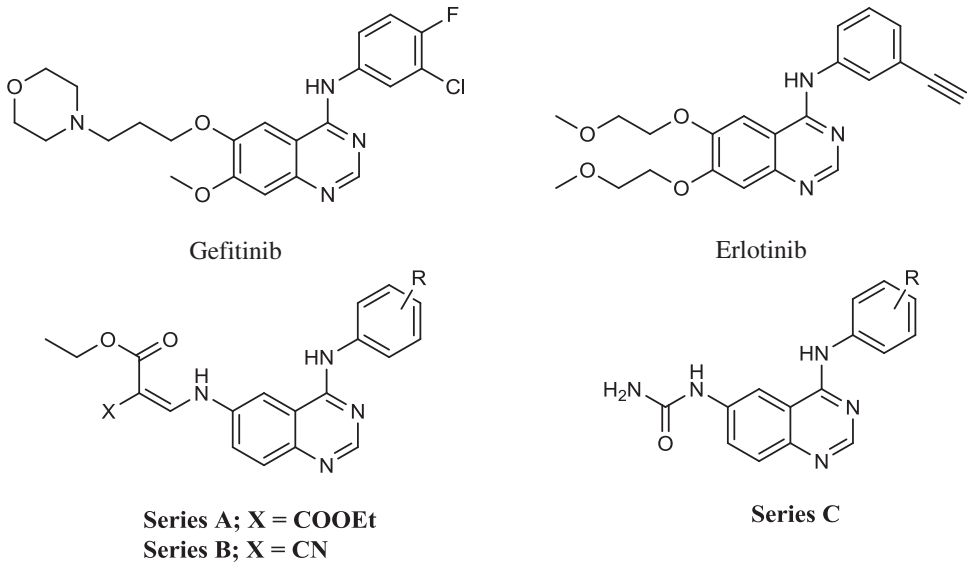

Fig. 1. Examples of EGFR receptor tyrosine kinase inhibitors and target compounds.

interaction with unique Cys-773 [20,21] as suggested by molecular modeling [22], and may also improve physical properties and impart a more favorable pharmacokinetics profile [17].

Encouraged by all these findings, we present three new series of 6-substituted 4-anilinoquinazolines as promising selective candidates for EGFR inhibition. Our strategy is directed toward designing a variety of ligands with diverse chemical properties hypothesizing that the potency and selectivity of these molecules might be enhanced by attaching new moieties at C-6 of substituted 4-anilinoquinazolines and/or by varying the aniline substitution pattern.

2. Rational and design

The design of our ligands was based on earlier work with quinazoline-based inhibitors of EGFR [9,17,23,24] and SAR studies on type I inhibitors of active EGFR [25]. Type I inhibitors are ATP competitive which bind to the hinge region of the enzymatically active kinase domain and represent the prototypical kinase inhibitor. In this study, three series of novel 6-substituted-quinazolines were designed to selectively inhibit EGFR, while preserving stereo electronic contacts responsible for binding to EGFR-TK. Accordingly, all the designed compounds incorporated the 4-anilinoquinazoline motif and derive selectivity through C-6 substitution with amino-2-cyanoacrylate **5**, aminomethylene malonate **6**, ureido **7** moieties. Where the conjugation in the enamine ester system (series A and B) and urea system (series C) directs the negative potential toward the carbonyl oxygen, which could lead to the formation of stronger hydrogen bonds and better affinity of these inhibitors in the active site, Also, different substitution pattern have been introduced at aniline in a fashion similar to gefitinib or erlotinib and finally phenolic hydroxyl group.

In this way, such substitution pattern could target additional regions of the ATP-binding site of the protein kinase domain to create differentially selective molecules. In addition, Genetic Optimization for Ligand Docking (GOLD) was used as flexible docking program [26] to predict the binding affinities and orientation of the target compounds **4b**, **5a**–**h**, **6a**–**f**, **7a**,**b** at the active site of the ATP binding site of EGFR-TK.

3. Chemistry

The route adopted for the synthesis of the new 6-substituted amino-4-anilinoquinazoline derivatives in this study is depicted in Schemes 1 and 2. The key intermediate 6-amino-4-anilinoquinazolines **4a**–**h**, were prepared following the literature methods [27–29] illustrated in Scheme 1. 6-Nitro-4-phenylaminoquinazoline derivatives **3a**–**h** were synthesized in good yield, through the reaction of 5-nitroanthranilo nitrile **1** with dimethylformamide dimethyl acetal affording the corresponding formamidine **2** followed by its reaction with appropriate anilines in acetic acid. Compounds **3a**–**h** were reduced to their amino derivatives using sodium dithionite in ammonia yielded the 6-aminoquinazolines **4a**–**h**.

(*Z*)-Ethyl 3-[4-(arylamino)quinazolin-6-ylamino]-2-cyanoacrylates **5a**–**h** were obtained as sole product, which was confirmed as *Z* isomer by means of low field signal of the NH-proton, where intramolecular H-bond between amino group and carbonyl group is accompanied by this deshielding effect [30]. Second, the H–N–CH coupling constants in this (*Z*) series are higher & less variable [31] with ^{1}H NMR of NH peak at 6-position of quinazoline appeared as doublet at δ 11.00–11.04 ppm (1H) with $J = 13.5$ Hz, that is coupled with proton of (NH–CH=C) with $J = 13.5$ Hz, moreover on adding D_2O (NH–CH=C) appeared as single peak δ at 8.44 ppm (1H), (*Z*)-ethyl 3-[4-(arylamino)quinazolin-6-ylamino]-2-cyanoacrylate **5a**–**h** were prepared by refluxing **4a**–**h** with (*E*)-ethyl 2-cyano-3-ethoxyacrylate in absolute ethanol. Also, their reaction with diethyl 2-(ethoxymethylene)malonate yielded diethyl 2-[(4-arylamino) quinazolin-6-ylaminomethylene]malonate **6a**–**f**. Finally, the reaction of the amino derivatives **4a**–**h** with potassium cyanate in acetic acid gave the corresponding 4-(substituted amino)-6-ureidoquinazoline **7a**,**b** Scheme 2.

4. Results and discussion

4.1. Pharmacology

4.1.1. In vitro EGFR tyrosine kinase activity

4.1.1.1. The initial screening effect. The EGFR tyrosine kinase assays were performed at BPS Bioscience (www.bpsbioscience.com). In the initial screening effect; the seventeen selected compounds indicated in Fig. 2 were tested over EGFR tyrosine kinase at a single dose concentration of 10 μM. At this concentration, compounds **5c**, **5d**, **5f**, **5g**, **6b**, **6d**, **6e**, **6g**, **7a**, and **7b** have demonstrated a significant inhibition of 100% for the activity EGFR tyrosine kinase, nevertheless the inhibition exerted by **4b**, **5a**, **5b**, **5e**, **5h** and **6c** were above

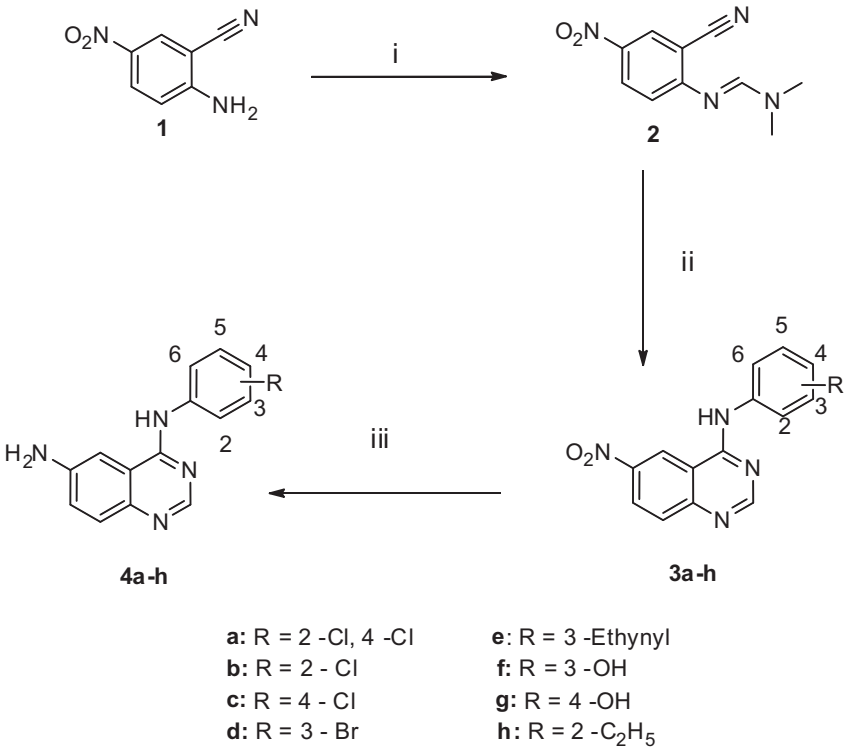

Scheme 1. Synthesis of 6-amino-4-anilinoquinazolines. Reagents and conditions: (i) dimethylformamide dimethyl acetal, 100 °C, 90 min; (ii) substituted aniline, glacial acetic acid, reflux, 60 min; (iii) sodium dithionite/ammonia, reflux.

80%. The mean percentage inhibition of the compounds on EGFR at the testing concentration (10 μM) was shown on Table 1, Fig. 2.

Structure–activity correlation of the newly synthesized 4-anilino-6-substituted aminoquinazolines derivatives revealed that the N substitution of the 6-amino group in the **4** series increased the inhibition percent in all the prepared final series (**5**,**6** and **7**). Combining these results together with preliminary gold docking scores, it was generally concluded that substitution at 6-position with ureido moiety (**7** series) results into the most active series followed by amino-methylene malonate moiety (**6** series), then the amino-2-cyanoacrylate moiety (**5** series). Moreover, for the 4-anilino ring substitution, we have introduced electron-withdrawing as halogen(s) and ethynyl group and electron-donating as ethyl, hydroxy function(s) to the 4-anilino ring. It was revealed that the 3-bromo (**5d** and **6d**), 3-hydroxy (**5f** and **7b**), 4-hydroxy (**5g** and **6f**), and 4-chloro (**5c** and **7a**) derivatives resulted into the highest inhibition percent for all the derivatives synthesized (100% inhibitions), However, the inhibition percent of the 4-chloro substituted derivative of amino-methylene malonate series (**6c**, 82%) revealed less inhibition percent than the corresponding **5** and **7** series derivatives (**5c** and **7a**). As for the rest of derivatives, 3-ethynyl (**5e**, **6e**), 2-chloro (**5b**, **6d**) and 2,4-dichloro (**5a**) showed inhibition percent range from (90–95%) and finally 2-ethyl derivative (**5h**) which was less potent than other compounds tested (84%). This study showed that the position and types of the substitutions affect the activity of the synthesized derivatives.

4.1.1.2. Measurement of potential enzyme inhibitory activity (IC_{50}). The profiling data for compound **7a** against EGFR showed increased inhibition of EGFR activity with increasing concentration of compound **7a** Fig. 3. The compound inhibited the EGFR activity by 99% at 10 μM, the IC_{50} value for **7a** was determined to be 0.061 μM, compared to that of gefitinib which is 0.033 μM.

4.1.2. Pharmacological (in vitro anticancer activity)

The structures of the final 4-anilino-quinazoline based products were submitted to National Cancer Institute "NCI" (www.dtp.nci.nih.gov), Bethesda, Maryland, USA, and six compounds were selected on the basis of degree of structure variation and computer modeling techniques for evaluation of their antineoplastic activity. The tumor growth inhibition properties of the six compounds **5a**, **5b**, **5c**, **5e**, **7a**, and **7b** with the NCI codes NSC D-757174/1, NSC D757173/1, D-757176/1, D-757175/1, D-757177/1, D-757178/1, selected among **5a**–**h**, **6a**–**f**, **7a**,**b** by the National Cancer Institute (NCI), USA, were screened on human tumor cell lines at 10^{-5} M, under the drug discovery program of the NCI. Among the selected six compounds, compound **7a** (NSC D-757177/1) was further screened for 5-log dose molar range due to its selective prominent cell growth inhibition on renal cell lines at 10^{-5} M concentration against verity of cell lines.

4.1.2.1. Primary single high dose (10^{-5} M) full NCI 60 cell panel in vitro assay. Primary *in vitro* one dose anticancer assay was performed in full NCI 60 cell panel. Results for each compound were reported as a mean graph of the percent growth of the treated cells when compared to the untreated control cells. Analysis of historical Development Therapeutics Programme (DTP) was performed and compound **7a** which satisfied predetermined threshold inhibition criteria was selected for NCI full panel 5 dose assays. The tested 4-anilino-quinazoline based inhibitors showed a distinctive pattern of selectivity & sensitivity against different NCI cell panel Table 2. Compound **7a** showed remarkably lowest cell growth promotion against breast cancer MDA-MB-468 cell line with cell growth promotion (7%). Compound **7a** exhibited broad spectrum cell growth inhibition against Non-Small Cell Lung Cancer NCI-H322M (cell growth promotion 18.02%, inhibition 81.98%), EKVX (cell growth promotion 22.36%, inhibition 77.64%), Ovarian SK-OV-3 (cell growth promotion 30.22%, inhibition 69.78%), Prostate

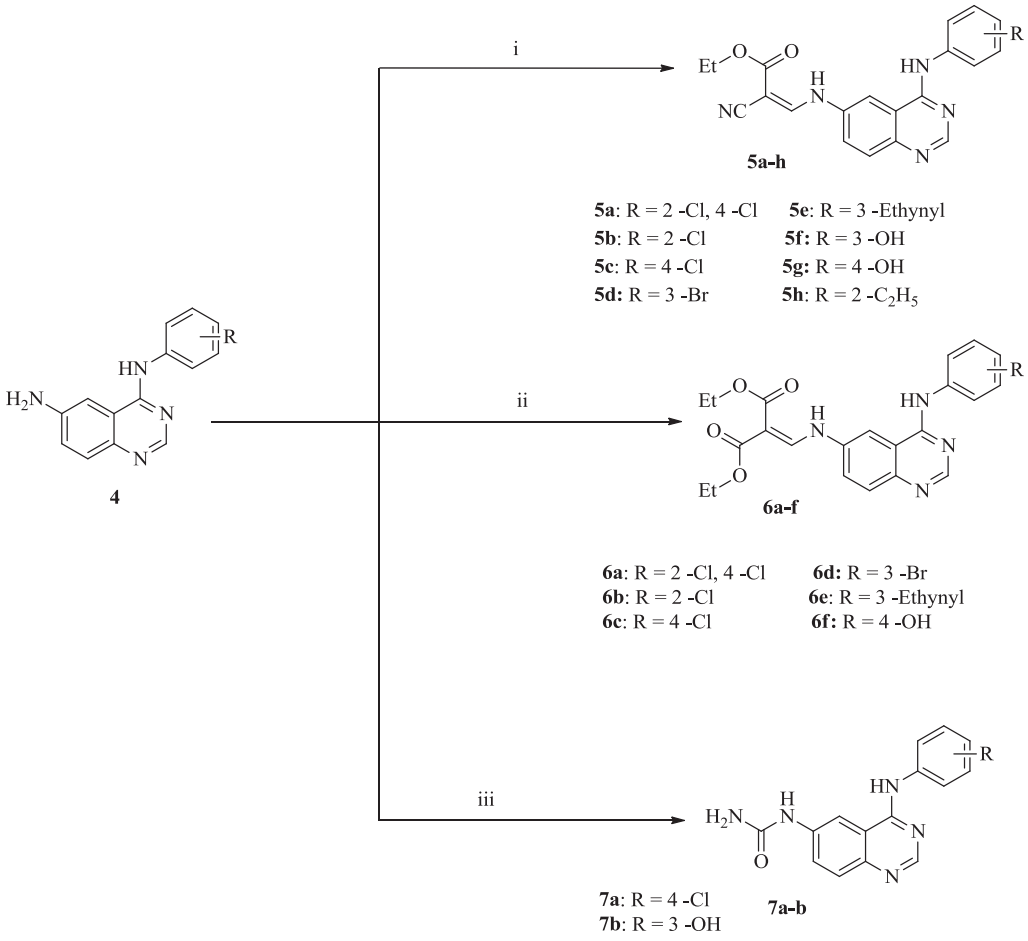

Scheme 2. Synthesis of 6-substituted amino-4-anilinoquinazolines. Reagents and conditions: (i) ethyl 2-cyano-3-ethoxyacrylate, abs. EtOH, reflux; (ii) diethyl 2-(ethoxymethylene)-malonate, abs. EtOH, reflux; (iii) KCNO, glacial acetic acid, stir on cold.

Cancer DU-145 (cell growth promotion 51.96%, inhibition 48.04%), Renal Cancer TK-10 (cell growth promotion 26.52%, inhibition 73.48%), CAKI-1 (cell growth promotion 40.11%, inhibition 59.98%), A498 (cell growth promotion 43.42%, inhibition 56.58%), ACHN (cell growth promotion 47.43%, inhibition 52.57%).

The second most active compound **5c** was found to be active against Non-Small Cell Lung Cancer EKVX (cell growth promotion 20.64%, inhibition 79.36%), NCI-H322M (cell growth promotion 22.61%, inhibition 77.39%), Renal Cancer CAKI-1 (cell growth

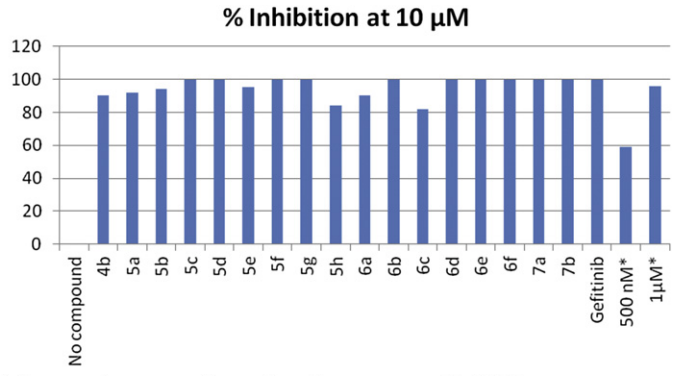

*: Staurosporine concentration, used as reference compound in EGFR enzyme assay

Fig. 2. The EGFR tyrosine kinase assay of synthesized compounds at a single dose concentration of 10 µM.

Table 1
The EGFR tyrosine kinase assays of the seventeen compounds over EGFR tyrosine kinase at a single dose concentration of 10 µM.

Compound	% Inhibition
4b	90[a]
5a	92[a]
5b	94[a]
5c	100[a]
5d	100[a]
5e	95[a]
5f	100[a]
5g	100[a]
5h	84[a]
6a	90[a]
6b	100[a]
6c	82[a]
6d	100[a]
6e	100[a]
6f	100[a]
7a	100[a]
7b	100[a]
Gefitinib	100[a]
Staurosporine	59[b]
Staurosporine	96[c]

[a] The inhibition % measured at 10 µM.
[b] The inhibition % measured at 0.5 µM.
[c] The inhibition % measured at 1 µM.

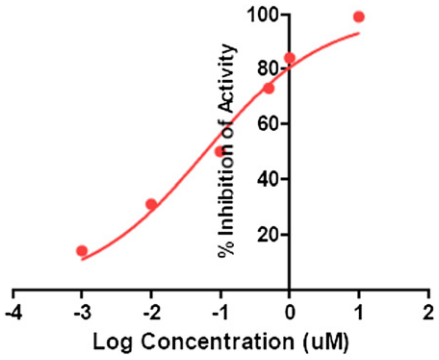

Fig. 3. Graph of **7a** Concentration against activity of EGFR; to determine IC_{50} value for **7a** to be 0.061 μM.

promotion 32.57%, inhibition 67.43%), UO-3 (cell growth promotion 42.95%, inhibition 57.05%), Breast Cancer MDA-MB-468 (cell growth promotion 26.64%, inhibition 73.36%), Prostate Cancer DU-145 (cell growth promotion 49.16%, inhibition 50.84%), Leukemia CCRF-CEM (cell growth promotion 50.08%, inhibition 49.92%), MOLT-4 (cell growth promotion 50.14%, inhibition 49.86%) and Ovarian Cancer OVCAR-3 cell line (cell growth promotion 50.23%, inhibition 49.77%). Contrary compound **7b** has not shown significant cell growth inhibition, while **5a** showed significant cell growth inhibition against Renal Cancer cell lines CAKI-1 (cell growth promotion 39.03%, inhibition 60.97%), UO-31 (cell growth promotion 42.02%, inhibition 57.98%), TK-10 (cell growth promotion 44.17%, inhibition 55.83%), A498 (cell growth promotion 48.72%, inhibition 51.28%), and against Non-Small Cell Lung EKVX Cancer cell line (cell growth promotion 41.70%, inhibition 58.3%). Compound **5b** is another active candidate which showed cell growth inhibition against Non-Small Lung EKVX (cell growth promotion 39.02%, inhibition 60.98%), Renal CAKI-1 (cell growth promotion 44.98%, inhibition 55.02%), Breast MDA-MB-468 cancer cell line (cell growth promotion 34.71%, inhibition 65.29%) and also showed up to 38% cell growth inhibition against Prostate DU-145 Cancer cell line. Compound **5e** emerged as active which cell growth inhibition against Non-Small Cell Lung EKVX (cell growth promotion was 31.89%, inhibition was 68.11%) and Breast MDA-MB-468 Cancer cell line (cell growth promotion was 40.41%, inhibition was 59.59%), moreover it also exhibited up to 44% cell growth inhibition against Renal CAKI-1 Cancer cell line at single dose assay (10^{-5} M concentration) as shown in Table 2.

4.1.2.2. In vitro 5 dose full NCI 60 cell panel assay. All the sixty cell lines, representing nine tumor subpanels, were incubated at five different concentrations (0.01, 0.1, 1, 10 &100 μM). The outcomes were used to create log concentration vs % growth inhibition curves and three response parameters (GI_{50}, TGI and LC_{50}) were calculated for each cell line, Table 3. The GI_{50} value (growth inhibitory activity) corresponds to the concentration of the compound causing 50% decrease in net cell growth, the TGI value (cytostatic activity) is the concentration of the compound resulting in total growth inhibition and LC_{50} value (cytotoxic activity) is the concentration of the compound causing net 50% loss of initial cells at the end of the incubation period of 48 h. Compound under investigation **7a** (NSC D-757177/1) exhibited remarkable anticancer activity against most of the tested cell lines representing nine different subpanels with GI_{50} values between "0.36–26.7 μM", except four cell lines of Colon Cancer subpanel namely COLO 205, HCC-2998, KM12 and SW-620 showed GI_{50} up to concentration of 27.5, 37.6, 28.4 and 39.7 μM respectively Table 3, note that compounds which were found to be insensitive at the highest tested concentration i.e. 100 mM

Table 2
Sixty human tumor cell line anticancer screening data at single dose assay (10^{-5} M concentration) as percent cell growth promotion of compounds **5a**, **5b**, **5c**, **5e**, **7a**, **7b**.

	5a	5b	5c	5e	7a	7b
Leukemia						
CCRF-CEM	70.92	93.13	50.08	103.42	96.01	107.99
HL-60 (TB)	107.69	95.26	76.22	97.46	99.87	105.04
K-562	59.67	88.59	61.38	96.37	71.44	103.44
MOLT-4	58.75	86.23	50.14	87.49	71.25	98.78
RPMI-8226	79.47	84.29	62.86	100.71	101.14	111.77
Non-small cell lung cancer						
A549/ATCC	72.08	82.40	66.13	85.06	72.48	93.49
EKVX	41.70	39.02	20.64	31.89	22.36	82.62
HOP-62	100.94	99.08	106.94	99.94	86.15	92.77
HOP-92	56.46	70.36	NT	90.30	74.20	77.99
NCI-H226	99.82	116.37	99.31	89.77	99.77	101.95
NCI-H23	99.50	103.48	92.49	98.23	100.15	100.38
NCI-H322M	75.65	46.95	22.61	52.30	18.02	83.53
NCI-H460	84.78	98.74	70.02	100.45	87.95	108.26
NCI-H522	95.79	107.01	79.75	86.31	66.20	102.48
Colon cancer						
COLO 205	107.97	110.19	102.45	103.55	101.41	94.71
HCC-2998	118.94	116.56	100.56	101.67	97.94	101.92
HCT-116	92.91	113.15	84.49	103.35	96.36	109.43
HCT-15	92.73	99.00	84.92	94.18	93.12	108.18
HT29	79.44	100.15	86.27	97.97	91.64	106.15
KM12	79.14	88.55	74.03	98.12	98.53	96.12
SW-620	100.49	115.97	97.35	105.31	99.11	99.10
CNS cancer						
SF-268	72.98	105.80	76.13	94.38	79.74	85.36
SF-295	82.15	101.83	74.26	95.57	90.72	98.11
SF-539	92.67	110.66	102.51	97.85	95.73	109.12
SNB-19	86.36	94.54	87.99	85.14	78.59	93.11
SNB-75	91.27	87.19	86.33	92.46	94.97	101.85
U251	81.35	96.35	84.68	85.41	95.72	87.85
Melanoma						
LOX IMVI	87.45	93.03	87.52	103.36	95.55	101.45
MALME-3M	140.24	156.12	141.92	119.27	117.44	120.67
M14	105.56	119.42	105.88	114.26	106.65	102.48
MDA-MB-435	75.74	100.26	70.46	92.03	97.83	101.34
SK-MEL-2	109.86	105.66	105.34	123.28	127.38	NT
SK-MEL-28	109.03	119.39	104.64	103.09	106.02	114.29
SK-MEL-5	78.35	88.32	71.99	89.38	89.20	100.77
UACC-257	97.16	120.30	107.96	99.77	100.15	99.82
UACC-62	90.03	107.31	102.89	103.87	87.90	105.04
Ovarian cancer						
IGROV1	55.03	79.74	52.40	77.41	61.01	107.40
OVCAR-3	67.63	95.27	50.23	78.68	74.21	82.83
OVCAR-4	95.07	124.09	89.00	94.05	91.88	112.27
OVCAR-5	82.20	90.06	92.75	89.52	83.64	98.14
OVCAR-8	87.03	104.89	83.33	94.82	89.54	98.87
NCI/ADR-RES	85.41	99.58	72.01	100.23	88.73	96.75
SK-OV-3	96.98	106.58	84.98	96.99	30.22	87.46
Renal cancer						
786-0	82.59	91.28	83.13	91.68	85.89	92.60
A498	48.72	63.73	53.12	82.55	43.42	77.40
ACHN	62.89	68.74	51.20	63.06	47.43	103.19
CAKI-1	39.03	44.98	32.57	56.14	40.11	84.79
RXF 393	77.05	91.72	83.18	92.86	93.70	110.60
SN12C	89.55	98.85	87.04	97.07	81.90	94.91
TK-10	44.17	53.02	51.34	65.47	26.52	103.01
UO-31	42.02	66.65	42.95	58.64	58.03	80.07
Prostate cancer						
PC-3	59.33	98.75	60.60	91.43	79.04	102.31
DU-145	55.92	62.12	49.16	69.86	51.96	90.36
Breast cancer						
MCF7	87.61	110.09	111.39	96.77	86.45	97.32
MDA-MB-231/ATCC	85.19	86.93	93.12	97.17	89.32	104.27
HS 578T	75.49	91.04	89.34	103.45	87.77	104.80
BT-549	89.56	112.43	76.06	99.56	92.36	108.27
T-47D	58.64	77.56	72.71	73.36	61.62	76.56
MDA-MB-468	56.36	34.71	26.64	40.41	−7.15	67.92

NT = Not tested, O 30–40% growth inhibition, O 40–50% growth inhibition, O 50–70% growth inhibition, O 70–90% growth inhibition, O 90–100% growth inhibition, O highly potent compound.

Table 3
NCI *in vitro* testing result of compound **7a** (NSC D-757177/1) at five dose level in μM.

Panel	Cell line	GI_{50}			TGI	LC_{50}
		Concentration per cell line	Subpanel MID[b]	Selectivity ratio (MID[a]:MID[b])		
Leukemia	CCRF-CEM	16.4	19.7	0.53	>100	>100
	HL-60 (TB)	24.4			69.8	>100
	MOLT-4	18.1			87.1	>100
	RPMI-8226	20.5			78.9	>100
	SR	19.1			75.6	>100
Non-small cell lung cancer	A549/ATCC	19.2	12.59	0.83	>100	>100
	EKVX	0.37			4.46	>100
	HOP-62	21.1			84.4	>100
	NCI-H226	22.3			>100	>100
	NCI-H322M	0.36			6.64	>100
	NCI-H460	22.4			>100	>100
	NCI-H522	2.40			20.9	>100
Colon cancer	COLO 205	27.5	28.56	0.367	>100	>100
	HCC-2998	37.6			>100	>100
	HCT-116	24.9			>100	>100
	HCT-15	17.8			>100	>100
	HT29	24.0			>100	>100
	KM12	28.4			>100	>100
	SW-620	39.7			>100	>100
CNS cancer	SF-268	17.1	15.61	0.67	>100	>100
	SF-295	14.8			45.5	>100
	SF-539	25.5			>100	>100
	SNB-19	9.02			>100	>100
	SNB-75	3.36			47.0	>100
	U251	23.9			>100	>100
Melanoma	LOX IMVI	19.3	19.5	0.54	68.7	>100
	MALME-3M	22.0			60.7	>100
	M14	25.0			76.0	>100
	MDA-MB-435	16.9			47.6	>100
	SK-MEL-2	15.1			42.7	>100
	SK-MEL-28	26.7			>100	>100
	SK-MEL-5	13.5			30.7	70.1
	UACC-257	23.5			75.2	>100
	UACC-62	13.5			32.2	77.0
Ovarian cancer	IGROV1	6.85	12.04	0.87	27.6	90.1
	OVCAR-3	8.36			69.5	>100
	OVCAR-4	9.14			>100	>100
	OVCAR-5	15.2			90.3	>100
	OVCAR-8	21.7			>100	>100
	NCI/ADR-RES	19.5			>100	>100
	SK-OV-3	3.52			20.5	>100
Renal cancer	786-0	20.7	6.91	1.51	88.9	>100
	A498	0.45			13.0	64.8
	ACHN	1.47			35.8	>100
	CAKI-1	1.33			21.5	>100
	RXF 393	15.1			75.9	>100
	SN12C	11.1			50.0	>100
	TK-10	0.98			16.2	>100
	UO-31	4.22			43.0	>100
Prostate cancer	PC-3	16.7	9.71	1.08	92.5	>100
	DU-145	2.72			>100	>100
Breast cancer	MCF7	26.2	12.61	0.83	>100	>100
	MDA-MB-231/ ATCC	8.92			37.7	>100
	HS 578T	14.8			55.9	>100
	BT-549	18.2			79.3	>100
	T-47D	6.47			72.3	>100
	MDA-MB-468	1.09			3.95	>100
MID[a]		10.47				

[a] MID = Average sensitivity of all cell line in μM.
[b] MID = Average sensitivity of all cell line of a particular subpanel in μM.

therefore a sign of ">" is used as prefix to the concentration. With regard to the sensitivity against some individual cell lines Table 3, the compound showed high activity against Non-Small Cell Lung Cancer EKVX (GI_{50} equal to 0.37 μM), NCI-H322M (GI_{50} equal to 0.36 μM), Renal Cancer A498 (GI_{50} equal to 0.46 μM), TK-10 (GI_{50} equal to 0.99 μM) and Breast Cancer MDA-MB-468 (GI_{50} equal to 1.096 μM) in which EGFR is over expressed [16,33,34]. Obtained data revealed an obvious sensitivity profile toward renal subpanel (GI_{50} value ranging from 0.46 to 20.7 μM), least for A498 and maximum for 786-0 cell line. Note that EGFR is over expressed in cancer cells of Non-Small Cell Lung Cancer, renal tumors, breast and hormone refractory prostate cancer [3–10].

The criterion for selectivity of a compound depends upon the ratio obtained by dividing the full panel MID (the average

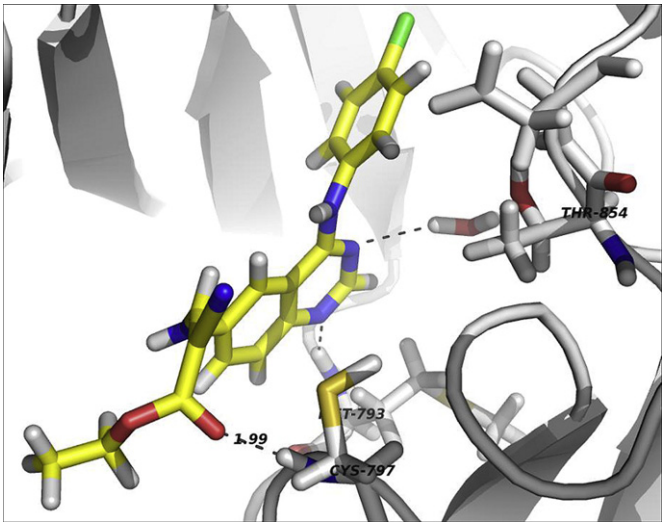

Fig. 4. Docking of compound **5c** (yellow carbons) in the ATP binding site of EGFR TK (PDB code 2J5F) in 3D style; showing key hydrogen bonding (dotted lines) between N-1 of quinazoline hydrogen bonds with Met769 NH and the N3 interacts with side chain of Thr766 through a water bridge. (For interpretation of the references to colour in this figure legend, the reader is referred to the web version of this article.)

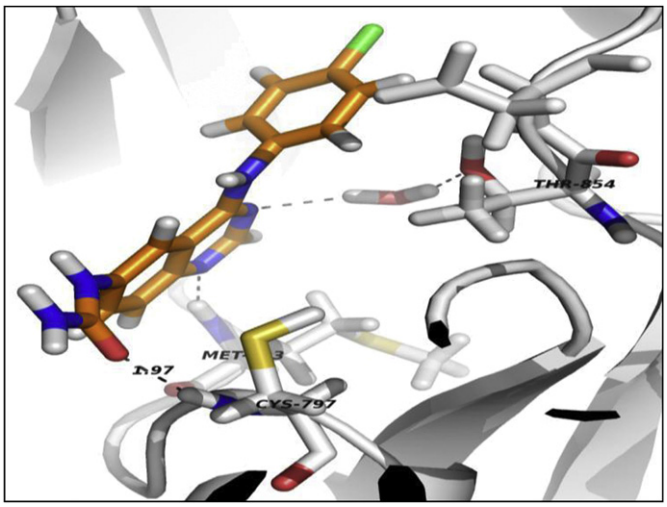

Fig. 6. Docking of compound **7a** in the ATP binding site of EGFR TK (PDB code 2J5F) in 3D style; showing key hydrogen bonding (dotted lines) between N-1 of quinazoline hydrogen bonds with Met769 NH and the N-3 interacts with side chain of Thr766 through a water bridge.

sensitivity of all cell lines toward the test agent) by their individual subpanel MID (the average sensitivity of all cell lines of a particular subpanel toward the test agent). As per this criterion, compound **7a** in the study was found to be most selective toward renal cancer subpanel, Table 3. Levels of EGFR mRNA and TGF-α (a ligand for EGFR) mRNA were highest in cell lines derived from renal cancers [33]. Thus on the basis of cytotoxicity patterns of these compounds we were able to support the original EGFR targeting strategy.

In addition to that, COMPARE analysis was performed; COMPARE is a computerized, pattern recognition algorithm which has considerable utility in the evaluation and exploitation of data generated by the NCI screen. In essence, COMPARE is a method of determining and expressing the degree of similarity, or lack thereof, of mean-graph profiles generated on the same or different compounds. Realization that compounds of either related or unrelated structures and matched by mean-graph patterns frequently shared the same or related biochemical mechanisms of action. Compound **7a** was chosen as a "seed" to search the NCI database for compounds of known mechanism with similar patterns of sensitivity, or for molecular targets, whose pattern of expression correlates with sensitivity to compound **7a**, thus generating hypotheses as to the mechanism of action of the novel compound that can be tested in the laboratory. Interestingly COMPARE analysis illustrates a high correlation between GI_{50} mean graph of compound **7a** with that of gefitinib & erlotinib to be 0.76 & 0.819, respectively which were reported as selective EGFR inhibitors [35], moreover the GI_{50} mean graph for renal & prostate cancer panel of relative high sensitivity against tested compound **7a**, when

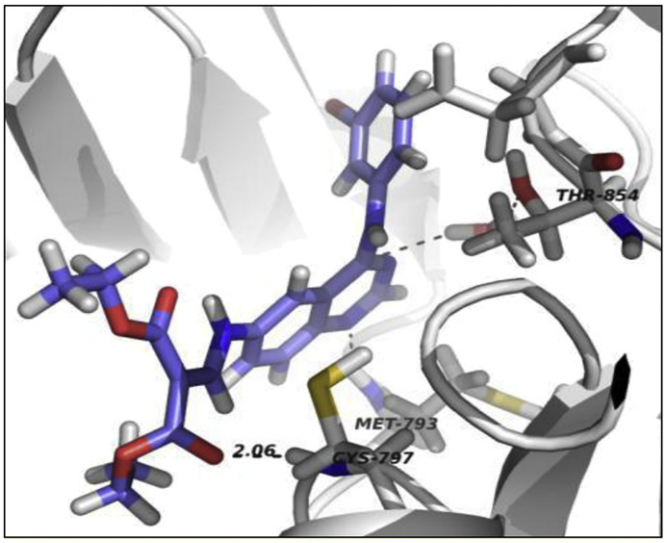

Fig. 5. Docking of compound **6d** in the ATP binding site of EGFR TK (PDB code 2J5F) in 3D style; showing key hydrogen bonding (dotted lines) between N-1 of quinazoline hydrogen bonds with Met769 NH and the N-3 interacts with side chain of Thr766 through a water bridge.

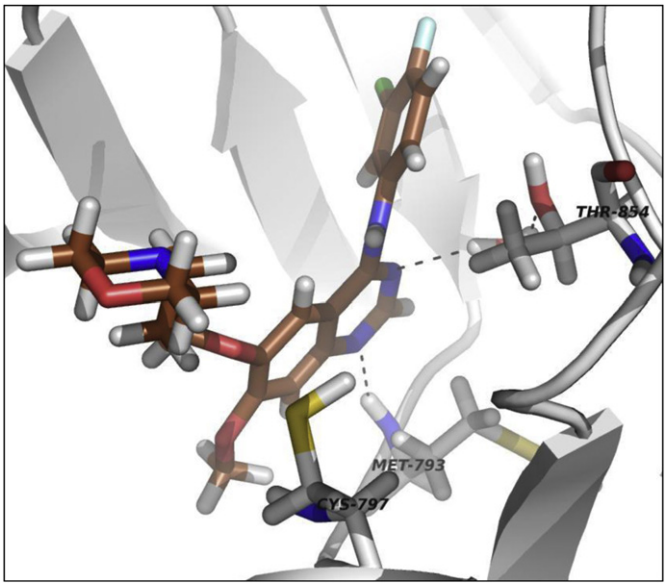

Fig. 7. Docking of gefitinib in the ATP binding site of EGFR TK (PDB code 2J5F) in 3D style; showing key hydrogen bonding (dotted lines) between N-1 of quinazoline hydrogen bonds with Met769 NH and the N-3 interacts with side chain of Thr766 through a water bridge.

compared with mean graph based on expression pattern of mRNA of EGFR in the cell lines of National Cancer Institute [33]. Both mean graphs are visually similar and the profile of cell line response was consistent with expected expression of EGFR; showing bars projecting to the right for both drug sensitivity and mRNA for the EGFR target.

4.2. Docking studies

Docking study using GOLD 4.1 [26] was performed. GOLD is a genetic algorithm based docking program that allows a wide range of flexibility for the ligand and the protein [36]. It is used to predict the binding modes and orientation of the synthesized compounds at the active site of the ATP binding site of EGFR-TK. The coordinates of the EGFR-TK structure were obtained from the crystal structure of EGFR with its inhibitor (PDB code 2J5F), which was chosen because of the interaction between the 6-substitution of the irreversible inhibitor to unique cys-793 of EGFR. The root mean square difference (RMSD) between the top docking pose and original crystallographic geometry was 1.45 Å. Nevertheless, further validation of docking algorithm was achieved by docking of the selected lead compound, gefitinib in the active site of EGFR kinase PDB (2J5F), this was found to retrieve the reported binding mode of gefitinib in the X-ray crystal structure of the active site of EGFR kinase PDB (2ITY), Fig. 7, where the N-1 atom of quinazoline interacts via H-bond with backbone NH of Met769 [37].The binding mode of the 4-anilinoquinazoline based inhibitors **5a**–**h**, **6a**–**g**, **7a**, **b** were in consistency with the proposed design and rational. One of the best-scored poses of compounds in **5**, **6**, **7** series is presented in Figs. 4–6, where the main interactions between the ligand **5c**, **6d**, **7a** respectively and the receptor can be observed and identified as following: (i) the N-1 atom of quinazoline interacted via H-bond with backbone NH of Met-769 (ii) the N-3 made water mediated H-bond to the side chain of Thr-766 (iii) the substituted 4-anilinoquinazoline lied in a deep pocket at the back of the ATP binding site. Moreover the carbonyl bond of ester (or urea) group made extra hydrogen bonding with cys-793 which was absent in reference compound gefitinib Fig. 7, which could enhance the binding affinity and fix the ligands in its position.

5. Conclusion

Compound **7a** showed remarkably lowest cell growth promotion against breast cancer MDA-MB-468 cell line and exhibited broad spectrum cell growth inhibition followed by compound **5c** which is the most active one in the **5** series showing highest percent mean growth inhibition over the whole cell panels tested and 100% EGFR-TK inhibition then **5a**, **5e**, **5b** and finally, **7b** which although it showed 100% enzyme inhibition but it was the least for cell line inhibition. Although it was reported that the presence of electron withdrawing lipophilic groups at the meta-position of aniline is favored for EGFR activity [32], both **5f**, **7b** have shown high interaction energy in docking studies which is further confirmed by 100% EGFR enzyme inhibition. As for compound **7b** which showed the least cell line inhibition, it may be because of the hydrophilic substitution of the 3-hydroxy group at 4-anilinoquinazoline scaffold which decreases log P (partition coefficient) of the compound decreasing penetration across cell membrane and hence its inhibition percent. Furthermore, compound **7a** was found to be the most selective candidate of the tested compounds at 5 dose level screening against cell lines which are of high EGFR expression [16,33,34], and obvious sensitivity profile toward renal subpanel, which has the highest expression levels of EGFR mRNA and TGF-a mRNA [33], also, renal subpanel showed highest selectivity ratio among all tested subpanels. Moreover, the selectivity profile was further confirmed through COMPARE analysis results. All these findings support EGFR targeting strategy and present **7a** as promising EGFR-TK inhibitor that can be further investigated to be used for a well-characterized tumor type that is highly expressing of targeted kinase.

According to these results, we can conclude that 4-chloro derivatives **7a**, **5c** appear to be the most interesting compounds among the newly synthesized and seem potentially attractive as antitumor agents. These preliminary encouraging results of biological screening done on the synthesized compounds could offer an excellent framework in this field that may lead to discovery of potent and selective antitumor agent.

6. Experimental protocols

6.1. Chemistry

Starting materials and reagents were purchased from Sigma–Aldrich. Melting points were recorded on Stuart Scientific apparatus and were uncorrected. FT-IR spectra were recorded on a Perkin–Elmer spectrophotometer. ^{1}H NMR spectra were recorded in δ scale given in ppm on a GEMINI-200 MHz spectrophotometer, or Varian Mercury VX-300 NMR spectrometer. Coupling patterns are described as follows: s, singlet; d, doublet, dd, doubled doublet; t, triplet; m, multiplet; and 1*H*, 2*H*, 3*H*, etc. *J* describes a coupling constant. The coupling constants were rounded off to one decimal place. MS spectra mass were recorded on Shimadzu GCMS-QP 5050A gas chromatograph mass spectrometer (70 eV). Elemental analyzes were performed at the Microanalytical Center, Cairo University.

6.1.1. (E)-N′-(2-Cyano-4-nitrophenyl)-N,N-dimethylimidoformamide (**2**)

5-Nitroanthranilonitrile **1** (5.00 g, 30.7 mmol) was refluxed in 20 ml dimethylformamide dimethyl acetal. After 90 min, the mixture was allowed to cool at room temperature. The solid was filtered off, washed with several portions of diethyl ether and dried to yield **2** as yellow crystals (6.50 g, 96.9%), mp 153–155 °C as reported [27,38].

6.1.2. General method for preparation of 6-nitro-4-arylaminoquinazoline (**3a**–**h**)

A mixture of *N*′-(2-cyano-4-nitrophenyl)-*N*,*N*-dimethylformamide (3.0 g, 13.7 mmol) and appropriate aniline (15.1 mmol) in glacial acetic acid was stirred and refluxed for about 2 h, reactions were monitored with TLC. After the reaction was completed the mixture was filtered while hot. The solid was washed with diethyl ether and dried to yield **3a**–**h** [27,38].

*6.1.2.1. 4-(2,4-Dichlorophenylamino)-6-nitroquinazoline (**3a**).* Yield 97% as yellow crystals, mp 256–258 °C. IR: (ν_{max}, cm^{-1}): 3406 (NH), 1618 (NO$_2$) cm^{-1}. ^{1}H NMR (300 MHz) (DMSO-d_6) δ: 7.53–7.77 (m, 3H, anilino Hs), 7.941 (d, 1H, quinazoline H$_8$), 8.56–8.59 (m, 2H, quinazoline H$_2$, H$_7$), 9.58 (s, 1H, quinazoline H$_5$), 10.63 (s, 1H, anilino–NH exchangeable by D$_2$O). MS: *m*/*z* (%): 334 (M$^+$ − 1, 11.98%), 335 (M$^+$, 4.72%), 336 (M$^+$ + 1, 7.93%), Anal. Calcd. for $C_{14}H_8Cl_2N_4O_2$: C 50.17, H 2.41, N 16.72; found: C 50.42, H 2.47, N 16.92.

*6.1.2.2. 4-(2-Chlorophenylamino)-6-nitroquinazoline (**3b**).* Yield 95% as yellow crystals, mp 180–182 °C. IR: (ν_{max}, cm^{-1}): 3359 (NH), 1617 (NO$_2$) cm^{-1}. ^{1}H NMR (300 MHz) (DMSO-d_6) δ: 7.38–7.62 (m, 4H, anilino H's), 7.93 (d, 1H, quinazoline H$_8$), 8.54–8.58 (m, 2H, quinazoline H$_2$, H$_7$), 9.59 (s, 1H, quinazoline H$_5$), 10.61 (s, 1H, anilino–NH exchangeable by D$_2$O). MS: *m*/*z* (%): 300.1 (M$^+$, 10.61%), 302

($M^+ + 2$, 4.21%), Anal. Calcd. for $C_{14}H_9ClN_4O_2$: C 55.92, H 3.02, N 18.63; found: C 56.31, H 3.15, N 18.85.

*6.1.2.3. 4-(4-Chlorophenylamino)-6-nitroquinazoline (**3c**).* Yield 87% as yellow crystals, mp 264 °C, (as reported) [27].

*6.1.2.4. 4-(3-Bromophenylamino)-6-nitroquinazoline (**3d**).* Yield 76.5% as yellow crystals, mp 267–270 °C, (as reported) [27,28,38].

*6.1.2.5. 4-(3-Ethynylphenylamino)-6-nitroquinazoline (**3e**).* Yield 95% as yellow crystals, mp 271–272 °C, (as reported) [29].

*6.1.2.6. 4-(3-Hydroxyphenylamino)-6-nitroquinazoline (**3f**).* Yield 89%, mp 306–308 °C. IR: (ν_{max}, cm^{-1}): 3737 (OH), 3381 (NH), 1540 (NO_2) cm^{-1}. ^1H NMR (300 MHz) (DMSO-d_6) δ: 7.17–7.28 (m, 3H, anilino H_2, H_4, H_6), 7.37–7.38 (m, 1H, anilino H_5), 7.92–7.95 (d, 1H, quinazoline H_8, J = 9.3 Hz), 8.54–8.57 (dd, 1H, quinazoline H_7, J = 9.3 Hz, J = 2.4 Hz), 8.71 (s, 1H, quinazoline H_2), 9.50 (s, 1H, OH exchangeable by D_2O), 9.67–9.68 (d, 1H, quinazoline H_5, J = 2.4 Hz), 10.32 (s, 1H, anilino–NH, exchangeable by D_2O). MS: m/z (%): 281.3 ($M^+ - 1$, 46.85%), 282.4 (M^+, 37%), 283.6 ($M^+ + 1$, 8.68%), Anal. Calcd. for $C_{14}H_{10}N_4O_3$: C 59.57, H 3.57, N 19.85; found: C 59.88, H 3.61, N 20.11.

*6.1.2.7. 4-(3-Hydroxyphenylamino)-6-nitroquinazoline (**3g**).* Yield 84%, mp 314 °C, (as reported) [39].

*6.1.2.8. 4-(2-Ethylphenylamino)-6-nitroquinazoline (**3h**).* Yield 92%, mp 178–80 °C. IR: (ν_{max}, cm^{-1}): 3332 (NH), 2959 (CH aliphatic), 1563 (NO_2) cm^{-1}. ^1H NMR (300 MHz) (DMSO-d_6) δ: 1.07–1.12 (t, 3H, –Ph–CH_2–$\underline{CH_3}$), 2.54–2.61 (q, 2H, Ph–$\underline{CH_2}$–CH_3), 7.29–7.39 (m, 4H, anilino Hs), 7.88–7.90 (d, 1H, quinazoline H_8, J = 9.3 Hz), 8.50–8.54 (dd, 2H, quinazoline H_2, H_7, J = 9.3 Hz, J = 2.4 Hz), 9.59–9.60 (d, 1H, quinazoline H_5, J = 2.4 Hz), 10.37 (s, 1H, anilino–NH, exchangeable by D_2O). MS: m/z (%): 294.4 (M^+, 31.21%), 296.7 ($M^+ + 2$, 0.51%) Anal. Calcd. for $C_{16}H_{14}N_4O_2$: C 65.30, H 4.79, N 19.04; found: C 65.62, H 4.82, N 19.12.

*6.1.3. General method for preparation of 6-amino-4-arylaminoquinazoline (**4a**–**h**)*

To a solution of compound **3** (3.42 g, 0.01 mol) in NH_4OH (20 ml, 30%), a solution of sodium dithionite (7 g, 0.04 mol) in water (30 ml) was quickly added, the reaction mixture was refluxed for 30 min. After cooling, the crude product was filtered off, washed and crystallized from ethanol [40].

*6.1.3.1. N^4-(2,4-Dichlorophenyl)-4,6-quinazolinediamine (**4a**).* Yield 80%, mp 244–246 °C. IR: (ν_{max}, cm^{-1}): 3415, 3385 (2 NH) cm^{-1}. ^1H NMR (300 MHz) (DMSO-d_6) δ: 5.62 (s, 2H, quinazoline–NH_2), 6.89–7.54 (m, 5H, anilino H_3, H_5, H_6, quinazoline H_5, H_7), 7.72–7.75 (m, 1H, quinazoline H_8), 8.27 (s, 1H, quinazoline H_2), 9.31 (s, 1H, anilino–NH, exchangeable by D_2O). MS: m/z (%): 303.9 ($M^+ - 1$, 22.6%), 304.95 (M^+, 8.97%), 305.9 ($M^+ + 1$, 13.97%), 306.9 ($M^+ + 2$, 3.87%) & base peak at 268.5 (100%) Anal. Calcd. for $C_{14}H_{10}Cl_2N_4$: C 55.10, H 3.30, N 18.36; found: C 55.23, H 3.35, N 18.45.

*6.1.3.2. N^4-(2-Chlorophenyl)quinazoline-4,6-diamine (**4b**).* Yield 75%, mp 269–271 °C. IR: (ν_{max}, cm^{-1}): 3415, 3854 (2 NH) cm^{-1}. ^1H NMR (300 MHz) (DMSO-d_6) δ: 5.62 (s, 2H, quinazoline–NH_2), 7.27–7.59 (m, 6H, anilino H_3, H_4, H_5, H_6 & quinazoline H_5, H_7), 7.62–7.75 (m, 1H, quinazoline H_8), 8.26 (s, 1H, quinazoline H_2), 9.28 (s, 1H, anilino–NH, exchangeable by D_2O). MS: m/z (%): 269.7 ($M^+ - 1$, 3.84%) 270.5 (M^+, 11.97%), 272.6 ($M^+ + 2$, 4.87%) & base peak at 51.5 (100%), Anal. Calcd. for $C_{14}H_{11}ClN_4$: C 62.11, H 4.1, N 20.7; found: C 62.28, H 4.15, N 20.8.

*6.1.3.3. N^4-(4-Chlorophenyl)quinazoline-4,6-diamine (**4c**).* Yield 88% as yellow crystals, mp 237–239 °C, (as reported) [38].

*6.1.3.4. N^4-(3-Bromophenyl)quinazoline-4,6-diamine (**4d**).* Yield 78%, mp 267–270 °C, (as reported) [27,28,38].

*6.1.3.5. N^4-(3-Ethynylphenyl)quinazoline-4,6-diamine (**4e**).* Yield 62%, mp 110–111 °C, (as reported) [29].

*6.1.3.6. N^4-(3-Hydroxyphenyl)quinazoline-4,6-diamine (**4f**).* Yield 80%, mp 197–199 °C. IR: (ν_{max}, cm^{-1}): 3520, 3357 (2 NH), 3224 (OH) cm^{-1}. ^1H NMR (300 MHz) (DMSO-d_6) δ: 5.6 (s, 2H, quinazoline–NH_2), 5.9–5.9 (dd, 1H, quinazoline H_7, J = 9 Hz, J = 2.4 Hz), 5.97–6.00 (m, 1H, quinazoline H_5, J = 2.4 Hz), 6.47–6.51 (m, 1H, anilino H_2), 7.15–7.26 (m, 2H, anilino H_4, H_6), 7.36–7.37 (m, 1H, anilino H_5), 7.50–7.53 (d, 1H, quinazoline H_8, J = 9 Hz), 8.34 (s, 1H, quinazoline H_2), 8.80 (s, 1H, phenol–OH, exchangeable by D_2O), 9.35 (s, 1H, anilino–NH, exchangeable by D_2O). MS: m/z (%): 251.3 ($M^+ - 1$, 35.35%), 252.5 (M^+, 18.72%) & base peak at 78 (100%), Anal. Calcd. for $C_{14}H_{12}N_4O$: C 66.65, H 4.79, N 22.2; found: C 66.71, H 4.82, N 22.31.

*6.1.3.7. N^4-(4-Hydroxyphenyl)quinazoline-4,6-diamine (**4g**).* Yield 83%, mp 192–194 °C. IR: (ν_{max}, cm^{-1}): 3402, 3350 (2 NH), 3226 (OH) cm^{-1}. ^1H NMR (300 MHz) (DMSO-d_6) δ: 5.61 (s, 2H, quinazoline–NH_2), 5.90–5.94 (dd, 1H, quinazoline H_7, J = 9 Hz, J = 2.4 Hz), 5.86–5.97 (m, 1H, quinazoline H_5, J = 2.4 Hz), 6.72–6.77 (m, 2H, anilino H_2, H_6), 7.35–7.57 (m, 2H, anilino H_3, H_5), 7.63–7.66 (d, 1H, quinazoline H_8, J = 9 Hz), 8.34 (s, 1H, quinazoline H_2), 8.56 (s, 1H, phenol–OH, exchangeable by D_2O), 9.42 (s, 1H, anilino–NH, exchangeable by D_2O). MS: m/z (%): 251.3 ($M^+ - 1$, 32.5%), 252.5 (M^+, 13.72%) & base peak at 77.9 (100%), Anal. Calcd. for $C_{14}H_{12}N_4O$: C 66.65, H 4.79, N 22.2; found: C 66.8, H 4.84, N 22.4.

*6.1.3.8. N^4-(2-Ethylphenyl)quinazoline-4,6-diamine (**4h**).* Yield 66%, mp 264–265 °C. IR: (ν_{max}, cm^{-1}): 3428, 3321 (2 NH), 2964 (CH) cm^{-1}. ^1H NMR (300 MHz) (DMSO-d_6) δ: 1.07–1.12 (t, 3H, CH_2–$\underline{CH_3}$), 2.54–2.61 (q, 2H, $\underline{CH_2}$–CH_3), 5.49 (s, 2H, quinazoline–NH_2, exchanged by D_2O), 7.20–7.33 (m, 6H, anilino H_3, H_4, H_s, H_6, quinazoline H_5, H_7), 7.47–7.50 (m, 1H, quinazoline H_8), 8.10 (s, 1H, quinazoline H_2), 9.08 (s, 1H, anilino–NH, exchangeable by D_2O). MS: m/z (%): 264.2 (M^+, 20.47%), 265.6 ($M^+ + 1$, 2.84%) & base peak at 89.85 (100%). Anal. Calcd. for $C_{16}H_{16}N_4$: C 72.7, H 6.1, N 21.2; found: C 72.89, H 6.18, N 21.43.

*6.1.4. General method for preparation of (Z)-ethyl 3-[4-(arylamino) quinazolin-6-ylamino]-2-cyanoacrylate (**5a**–**h**)*

To a solution (0.01 mol) of appropriate amine in absolute ethanol, (*Z*)-ethyl 2-cyano-3-ethoxyacrylate (1.7 g, 0.01 mol) was added, the reaction mixture was refluxed about 3 h. After cooling, the crude product was filtered off, washed and crystallized from ethanol.

*6.1.4.1. (Z)-Ethyl 3-[4-(2,4-dichlorophenylamino)quinazolin-6-ylamino]-2-cyanoacrylate (**5a**).* Yield 85%, mp 155–156 °C. IR: (ν_{max}, cm^{-1}): 3402, 3294 (2 NH), 2218 (CN), 3194 (aliphatic CH), 1678 (CO), 1624 (vinyl C=C) cm^{-1}. ^1H NMR (300 MHz) (DMSO-d_6) δ: 1.245–1.32 (t, 3H, –O–CH_2–$\underline{CH_3}$), 4.23–4.30 (q, 2H, –O–$\underline{CH_2}$–CH_3), 7.50–7.52 (m, 1H, anilino H_6), 7.55–7.61 (m, 1H, anilino H_5), 7.61–7.64 (m, 1H, anilino H_3), 7.79 (d, 1H, quinazoline H_8), 8.01 (d, 1H, quinazoline H_7), 8.31 (d, 1H, quinazoline H_5), 8.51–8.57 (m, 1H, NH–$\underline{CH}$=C), 8.63 (s, 1H, quinazoline H_2), 9.73 (s, 1H, anilino–NH, exchangeable by D_2O), 11.02 (d, 1H, quinazoline–NH, exchangeable by D_2O). MS: m/z (%): 426.9 ($M^+ - 1$, 27.43%), 427.9 (M^+, 16.84%), 428.9 ($M^+ + 1$, 9.62%), 430 ($M^+ + 2$, 9.6%) & base peak at 346 (100%). Anal. Calcd. for $C_{20}H_{15}Cl_2N_5O_2$: C 56.09, H 3.53, N 16.35; found: C 56.18, H 3.63, N 16.39.

*6.1.4.2. (Z)-Ethyl 3-[4-(2-chlorophenylamino)quinazolin-6-ylamino]-2-cyanoacrylate (**5b**).* Yield 82%, mp 147–149 °C. IR: (ν_{max}, cm^{-1}): 3429, 3371 (2 NH), 2214 (CN), 2924, 2954 (aliphatic CH), 1678 (CO), 1643 (vinyl C=C) cm^{-1}. ^1H NMR (300 MHz) (DMSO-d_6) δ: 1.24–1.30 (t, 3H, –O–CH_2–$\underline{CH_3}$), 4.19–4.29 (q, 2H, –O–$\underline{CH_2}$–CH_3), 7.34–7.48 (m, 2H, anilino H_6, H_4) 7.57–7.628 (m, 2H, anilino H_3, H_5), 7.77–7.82 (m, 1H, quinazoline H_8, J = 9 Hz), 7.91–8.07 (dd, 1H, quinazoline H_7, J = 9 Hz, J = 2.4 Hz), 8.40–8.42 (m, 1H, quinazoline H_5, J = 2.4 Hz), 8.46–8.60 (m, 2H, quinazoline H_2, NH–$\underline{CH}$=C), 9.69 (s, 1H, anilino–NH exchangeable by D_2O), 10.98–11.02 (d, 1H, quinazoline–NH, exchangeable by D_2O). MS: *m*/*z* (%): 393 (M^+, 72.5%), 395 (M^+ + 2, 43.75%) & base peak at 281 (100%), Anal. Calcd. for $C_{20}H_{16}ClN_5O_2$: C 60.99, H 4.09, N 17.78; found: C 61.12, H 4.18, N 17.97.

*6.1.4.3. (Z)-Ethyl 3-[4-(4-chlorophenylamino)quinazolin-6-ylamino]-2-cyanoacrylate (**5c**).* Yield 86%, mp 255–257 °C. IR: (ν_{max}, cm^{-1}): 3429, 3371 (2 NH), 2214 (CN), 2978 (aliphatic CH), 1678 (CO), 1628 (vinyl C=C) cm^{-1}. ^1H NMR (300 MHz) (DMSO-d_6) δ: 1.25–1.32 (t, 3H, –O–CH_2–$\underline{CH_3}$), 4.20–4.31 (q, 2H, –O–$\underline{CH_2}$–CH_3), 7.45–7.48 (m, 2H, anilino H_2, H_6), 7.77–7.80 (m, 1H, quinazoline H_8, J = 9 Hz), 7.86 (d, 2H, quinazoline H_3, H_5), 7.90–8.05 (dd, 1H, quinazoline H_7, J = 9 Hz, J = 2.4 Hz), 8.38–8.42 (d, 1H, quinazoline H_5, J = 2.4 Hz), 8.50–8.60 (m, 2H, quinazoline H_2, NH–$\underline{CH}$=C), 9.71 (s, 1H, anilino–NH exchangeable by D_2O), 10.98–11.03 (d, 1H, quinazoline–NH, exchangeable by D_2O). MS: *m*/*z* (%): 393.5 (M^+, 71.04%), 395.5 (M^+ + 2, 29.8%), Anal. Calcd. for $C_{20}H_{16}ClN_5O_2$: C 60.99, H 4.09, N 17.78; found: C 61.42, H 4.14, N 18.12.

*6.1.4.4. (Z)-Ethyl 3-[4-(3-bromophenylamino)quinazolin-6-ylamino]-2-cyanoacrylate (**5d**).* Yield 70%, mp 188–190 °C. IR: (ν_{max}, cm^{-1}): 3549, 3325 (2 NH), 2214 (CN), 2989, 2939 (aliphatic CH), 1678 (CO), 1627 (vinyl C=CH) cm^{-1}. ^1H NMR (300 MHz) (DMSO-d_6) δ: 1.28–1.33 (t, 3H, –O–CH_2–$\underline{CH_3}$), 4.23–4.29 (q, 2H, –O–$\underline{CH_2}$–CH_3), 7.31–7.41 (m, 2H, anilino H_5, H_6), 7.79–7.83 (d, 1H, quinazoline H_8, J = 9 Hz), 7.85–7.90 (m, 1H, anilino H_4), 7.92–8.08 (dd, 1H, quinazoline H_7, J = 9 Hz, J = 2.4 Hz), 8.18–8.20 (d, 1H, anilino H_2), 8.40–8.43 (d, 1H, quinazoline H_5, J = 2.4 Hz), 8.55–8.59 (d, 1H, NH–$\underline{CH}$=C, J = 13.5 Hz), 8.61 (s, 1H, quinazoline H_2), 9.70 (s, 1H, anilino–NH exchangeable by D_2O), 11.00–11.04 (d, 1H, quinazoline–NH, exchangeable by D_2O, J = 13.5 Hz). ^{13}C NMR δ (ppm): 166.72, 165.02, 153.7, 153.03, 147.44, 141.17, 138.38, 137.05, 130.82, 129.45, 126.65, 124.84, 121.33, 118.47, 115.92, 109.53, 108.93, 75.19, 61.11, 14.71, MS: *m*/*z* (%): 438 (M^+, 8.8%), 439 (M^+ + 1, 8.79%), 440 (M^+ + 2, 82.36%), 441 (M^+ + 3, 28.09%), Anal. Calcd. for $C_{20}H_{16}BrN_5O_2$: C 54.8, H 3.68, N 15.98; found: C 55.02, H 3.72, N 15.68.

*6.1.4.5. (E)-Ethyl 3-[4-(3-ethynylphenylamino)quinazolin-6-ylamino]-2-cyanoacrylate (**5e**).* Yield 91%, mp 383–384 °C. IR: (ν_{max}, cm^{-1}): 3549, 3271 (2 NH), 2214 (CN), 2985 (aliphatic CH), 1678 (CO), 1635 (vinyl C=C) cm^{-1}. ^1H NMR (300 MHz) (DMSO-d_6) δ: 1.25–1.32 (t, 3H, –O–CH_2–$\underline{CH_3}$), 4.21 (s, 1H, ethynyl CH), 4.22–4.32 (q, 2H, –O–$\underline{CH_2}$–CH_3), 7.26–7.29 (m, 1H, anilino H_6), 7.42–7.48 (m, 1H, anilino H_2), 7.79–7.82 (d, 1H, quinazoline H_8, J = 9 Hz), 7.88–7.95 (m, 1H, anilino H_4), 7.97–8.00 (m, 1H, anilino H_5), 8.04–8.11 (dd, 1H, quinazoline H_7, J = 9 Hz), 8.42–8.47 (m, 1H, quinazoline H_5), 8.58 (d, 1H, NH–$\underline{CH}$=C), 8.63 (s, 1H, quinazoline H_2), 9.81 (s, 1H, anilino–NH, exchangeable by D_2O), 11.02–11.06 (d, 1H, quinazoline–NH, exchangeable by D_2O). MS: *m*/*z* (%): 381 (M^+ – 2, 8.99%), 383 (M^+, 7.96%), Anal. Calcd. for $C_{22}H_{17}N_5O_2$: C 68.9, H 4.47, N 18.27; found: C 69.2, H 4.51, N 18.31.

*6.1.4.6. (Z)-Ethyl 3-[4-(3-hydroxyphenylamino)quinazolin-6-ylamino]-2-cyanoacrylate (**5f**).* Yield 77%, mp 271–272.5 °C. IR: (ν_{max}, cm^{-1}): 3429, 3371 (2 NH), 3156 (OH) 2214 (CN), 2990 (aliphatic CH), 1678 (CO), 1635 (vinyl C=C) cm^{-1}. ^1H NMR (300 MHz) (DMSO-d_6) δ: 1.25–1.30 (t, 3H, –O–CH_2–$\underline{CH_3}$), 4.22–4.29 (q, 2H, –O–$\underline{CH_2}$–CH_3), 6.55–6.59 (m, 1H, anilino H_2), 7.16–7.26 (m, 2H, anilino H_4, H_6), 7.35–7.40 (m, 1H, anilino H_5), 7.76–7.80 (d, 1H, quinazoline H_8, J = 9 Hz), 7.89–8.05 (dd, 1H, quinazoline H_7, J = 9 Hz, J = 2.4 Hz), 8.41–8.47 (d, 1H, quinazoline H_5, J = 2.4 Hz), 8.54–8.58 (d, 1H, NH–$\underline{CH}$=C, J = 13.2 Hz), 8.60 (s, 1H, quinazoline H_2), 9.44 (s, 1H, OH exchangeable by D_2O), 9.69 (s, 1H, anilino–NH exchangeable by D_2O), 10.99–11.03 (d, 1H, quinazoline–NH, exchangeable by D_2O, J = 13.2 Hz). MS: *m*/*z* (%): 375.3 (M^+, 85.38%), 377.1 (M^+ + 2, 7.01%) & base peak at 45.9 (100%), Anal. Calcd. for $C_{20}H_{17}N_5O_3$: C 63.99, H 4.56, N 18.66; found: C 64.27, H 4.9, N 18.9.

*6.1.4.7. (Z)-Ethyl 3-[4-(4-hydroxyphenylamino)quinazolin-6-ylamino]-2-cyanoacrylate (**5g**).* Yield 88%, mp 260–261.5 °C. IR (ν_{max}, cm^{-1}): 3429, 3371 (2 NH), 3267 (OH), 2214 (CN), 3000 (aliphatic CH), 1678 (CO), 1627 (vinyl C=C) cm^{-1}. ^1H NMR (300 MHz) (DMSO-d_6) δ: 1.21–1.28 (t, 3H, –O–CH_2–$\underline{CH_3}$), 4.18–4.25 (q, 2H, –O–$\underline{CH_2}$–CH_3), 6.79–6.82 (d, 2H, anilino H_2, H_6), 7.42–7.48 (m, 2H, anilino H_3, H_5), 7.71–7.74 (d, 1H, quinazoline H_8, J = 9 Hz), 7.81–7.89 (dd, 1H, quinazoline H_7, J = 9 Hz, J = 1.8 Hz), 8.27–8.33 (d, 1H, quinazoline H_5, J = 1.8 Hz), 8.38–8.44 (m, 1H, NH–$\underline{CH}$=C), 8.56 (s, 1H, quinazoline H_2), 9.49 (s, 1H, phenolic–OH, exchangeable by D_2O), 9.66 (s, 1H, anilino–NH exchangeable by D_2O), 10.95–11.01 (d, 1H, quinazoline–NH exchangeable by D_2O). MS: *m*/*z* (%): 375.5 (M^+, 70.84%), 377 (M^+ + 2, 7.84%), 378 (M^+ + 3, 1.25%) & base peak at 328.5 (100%), Anal. Calcd. for $C_{20}H_{17}N_5O_3$: C 63.99, H 4.56, N 18.66; found: C 64.50, H 4.69, N 18.93.

*6.1.4.8. (Z)-Ethyl 3-[4-(2-ethylphenylamino)quinazolin-6-ylamino]-2-cyanoacrylate (**5h**).* Yield 84%, mp 198.5–200.5 °C. IR (ν_{max}, cm^{-1}): 3429, 3371 (2 NH), 2214 (CN), 2970, 2933 (aliphatic CH), 1678 (CO), 1629 (vinyl C=C) cm^{-1}. ^1H NMR (300 MHz) (DMSO-d_6) δ: 1.07–1.12 (t, 3H, –Ph–CH_2–$\underline{CH_3}$), 1.24–1.32 (t, 3H, –O–CH_2–$\underline{CH_3}$), 2.49–2.51 (q, 2H, –Ph–$\underline{CH_2}$–CH_3), 4.18–4.31 (q, 2H, –O–$\underline{CH_2}$–CH_3), 7.29–7.32 (m, 3H, anilino H_4, H_5, H_6), 7.35–7.39 (m, 1H, anilino H_3), 7.74–7.78 (d, 1H, quinazoline H_8, J = 9 Hz), 7.96 (d, 1H, quinazoline H_7, J = 9 Hz), 8.33–8.42 (m, 1H, quinazoline H_5), 8.44–8.45 (m, 1H, NH–$\underline{CH}$=C), 8.61 (s, 1H, quinazoline H_2), 9.73 (s, 1H, anilino–NH exchangeable by D_2O) , 10.98 (d, 1H, quinazoline–NH, exchangeable by D_2O). MS: *m*/*z* (%): 388 (M^+, 100%), 389 (M^+ + 1, 21.7%), 390 (M^+ + 2, 1.93%), Anal. Calcd. for $C_{22}H_{21}N_5O_2$: C 68.2, H 5.46, N 18.08; found: C, H, N (C 68.33, H 5.47, N 18.09).

*6.1.5. General method for preparation of diethyl 2-[(4-arylamino) quinazolin-6-ylaminomethylene]malonate (**6a**–**f**)*

A mixture of appropriate amine (0.01 mol) & diethyl 2-(ethoxymethylene)malonate (2.16 g, 0.01 mol) in absolute ethanol was refluxed about 2 h. After cooling, the crude product was filtered off, washed and crystallized from ethanol.

*6.1.5.1. Diethyl 2-[(2,4-dichlorophenylamino)quinazolin-6-ylaminomethylene]malonate (**6a**).* Yield 95%, mp 280.6–282.7 °C. IR: (ν_{max}, cm^{-1}): 3412 cm^{-1} (NH), 2923 cm^{-1} (aliphatic CH), 1680 (CO), 1640 (vinyl C=C) cm^{-1}. ^1H NMR (300 MHz) (DMSO-d_6) δ: 1.24–1.31 (2t, 6H, 2× –O–CH_2–$\underline{CH_3}$), 4.14–4.28 (2q, 4H, 2× –O–$\underline{CH_2}$–CH_3), 7.50–7.51 (m, 1H, anilino H_6), 7.53–7.56 (m, 1H, anilino H_5), 7.61–7.64 (m, 1H, anilino H_3), 7.78–7.82 (d, 1H, quinazoline H_8, J = 9 Hz), 7.94–8.04 (d, 1H, quinazoline H_7, J = 9 Hz), 8.40 (d, 1H, quinazoline H_5), 8.57–8.61 (d, 1H, NH–$\underline{CH}$=C, J = 13.5 Hz), 8.42 (s, 1H, quinazoline H_2), 9.89 (s, 1H, anilino–NH exchangeable by D_2O), 10.95–10.99 (d, 1H, quinazoline–NH, exchangeable by D_2O, J = 13.5 Hz). MS: *m*/*z* (%): 475 (M^+, 10%), 476 (M^+ + 1, 7.25%), 478.15

(M^+ + 3, 1.31%) & base peak at 45.9 (100%), Anal. Calcd. for $C_{22}H_{20}Cl_2N_4O_4$: C 55.6, H 4.24, N 11.79; found: C 55.83, H 4.31, N 11.98.

*6.1.5.2. Diethyl 2-[(2-chlorophenylamino) quinazolin-6-ylaminomethylene]malonate (**6b**).* Yield 98%, mp 130–132 °C. IR: (ν_{max}, cm^{-1}): 3560 (NH), 2981 (aliphatic CH), 1698 (CO), 1603 (vinyl C=C) cm^{-1}. ^1H NMR (300 MHz) (DMSO-d_6) δ: 1.24–1.31 (2t, 6H, 2× –O–CH_2–CH_3), 4.14–4.29 (2q, 4H, 2× –O–CH_2–CH_3), 7.36–7.47 (m, 2H, anilino H_6, H_4), 7.57–7.62 (m, 2H, anilino H_3, H_5), 7.79–7.82 (d, 1H, quinazoline H_8, J = 9 Hz), 7.92–8.96 (dd, 1H, quinazoline H_7, J = 9 Hz, J = 2.4 Hz), 8.39–8.40 (d, 1H, quinazoline H_5, J = 2.4 Hz), 8.42 (s, 1H, quinazoline H_2), 8.58–8.62 (d, 1H, NH–CH=C, J = 13.5 Hz), 9.87 (s, 1H, anilino–NH, exchangeable by D_2O), 10.95–10.99 (d, 1H, quinazoline–NH, exchangeable by D_2O, J = 13.5 Hz). MS: m/z (%): 440.8 (M^+, 71.43%), 442.7 (M^+ + 2, 33.94%), Anal. Calcd. for $C_{22}H_{21}ClN_4O_4$: C 59.93, H 4.8, N 12.71; found: C 59.58, H 4.53, N 12.59.

*6.1.5.3. Diethyl 2-[(4-dichlorophenylamino) quinazolin-6-ylaminomethylene]malonate (**6c**).* Yield 97%, mp 147–149 °C. IR: (ν_{max}, cm^{-1}): 3452 (NH), 2985, 2935 (aliphatic CH), 1686 (CO), 1647 (vinyl C=C) cm^{-1}. ^1H NMR (300 MHz) (DMSO-d_6) δ: 1.25–1.32 (2t, 6H, 2× –O–CH_2–CH_3), 4.14–4.29 (2q, 4H, 2× –O–CH_2–CH_3), 7.45–7.48 (d, 2H, anilino H_2, H_6), 7.79–7.82 (d, 1H, quinazoline H_8, J = 9 Hz), 7.89–7.92 (m, 2H, quinazoline H_3, H_5), 7.93–7.97 (dd, 1H, quinazoline H_7, J = 9 Hz, J = 2.4 Hz), 8.40–8.401 (d, 1H, quinazoline H_5, J = 2.4 Hz), 8.56 (s, 1H, quinazoline H_2), 8.57–8.616 (d, 1H, NH–CH=C, J = 13.5 Hz), 9.83 (s, 1H, anilino–NH exchangeable by D_2O), 10.99–11.04 (d, 1H, quinazoline–NH, exchangeable by D_2O, J = 13.5 Hz). MS: m/z (%): 440.8 (M^+, 40.64%), 442.6 (M^+ + 1, 20.25%), 444.1 (M^+ + 3, 1.86%) & base peak at 394.65 (100%), Anal. Calcd. for $C_{22}H_{21}ClN_4O_4$: C 59.93, H 4.8, N 12.71; found: C 59.6, H 4.77, N 12.52.

*6.1.5.4. Diethyl 2-[(3-bromophenylamino) quinazolin-6-ylaminomethylene]malonate (**6d**).* Yield 96%, mp 133–135 °C. IR: (ν_{max}, cm^{-1}): 3568 (NH), 3094 (aliphatic CH), 1686 (CO), 1640 (vinyl C=C) cm^{-1}. ^1H NMR (300 MHz) (DMSO-d_6) δ: 1.25–1.38 (2t, 6H, 2× –O–CH_2–CH_3), 4.15–4.29 (2q, 4H, 2× –O–CH_2–CH_3), 7.30–7.34 (m, 1H, anilino H_6), 7.36–7.41 (m, 1H, anilino H_5), 7.81–7.84 (d, 1H, quinazoline H_8, J = 9 Hz), 7.90 (d, 1H, anilino H_4), 7.95–8.99 (dd, 1H, quinazoline H_7, J = 9 Hz, J = 2.4 Hz), 7.99–8.02 (m, 1H, anilino H_2), 8.21–8.22 (d, 1H, quinazoline H_5, J = 2.4 Hz), 8.41 (s, 1H, quinazoline H_2), 8.58–8.62 (d, 1H, NH–CH=C, J = 13.5 Hz), 9.85 (s, 1H, anilino–NH exchangeable by D_2O), 10.99–11.04 (d, 1H, quinazoline NH, exchangeable by D_2O, J = 13.5 Hz). MS: m/z (%): 483 (M^+ − 2, 46.9%), 484 (M^+ − 1, 42%), 485 (M^+, 35.8%), 486 (M^+ + 1, 59.3%), Anal. Calcd. for $C_{22}H_{21}BrN_4O_4$: C 54.44, H 4.36, N 11.54; found: C 54.14, H 4.27, N 11.25.

*6.1.5.5. Diethyl 2-[(3-ethynylphenylamino) quinazolin-6-ylaminomethylene]malonate (**6e**).* Yield 96%, mp 274–276 °C. IR: (ν_{max}, cm^{-1}): 3440 (NH), 3229 (aliphatic CH), 1678 (CO), 1636 (vinyl C=C) cm^{-1}. ^1H NMR (300 MHz) (DMSO-d_6) δ: 1.25–1.31 (2t, 6H, 2× –O–CH_2–CH_3), 4.14 (s, 1H, ethynyl CH), 4.17–4.26 (2q, 4H, 2× –O–CH_2–CH_3), 7.25–7.30 (m, 1H, anilino H_6), 7.42–7.47 (m, 1H, anilino H_2), 7.80 -7.83 (m, 1H, quinazoline H_8), 7.94–7.97 (m, 1H anilino H_4), 7.97–8.01 (m, 1H, anilino H_5), 8.04–8.10 (dd, 1H, quinazoline H_7, J = 9 Hz, J = 2.4 Hz), 8.40–8.41 (d, 1H, quinazoline H_5, J = 2.4 Hz), 8.57 (s, 1H, quinazoline H_2), 8.59–8.64 (d, 1H, NH–CH=C), 9.81 (s, 1H, anilino–NH exchangeable by D_2O), 11.02–11.05 (d, 1H, quinazoline–NH, exchangeable by D_2O). ^{13}C NMR δ (ppm): 170.55, 158.57, 156.95, 152.18, 150.29, 139.84, 139.60, 129.83, 129.50, 125.67, 123.47, 124.84, 123.42, 122.36, 120.96, 109.38, 106.12, 84.00, 83.92, 81.21, 60.46, 56.18, 55.01, 14.82, 14.68.

MS: m/z (%): 430 (M^+, 52%), 431 (M^+ + 1, 19%), 432 (M^+ + 2, 4.1%) & base peak at 383 (100%), Anal. Calcd. for $C_{24}H_{22}N_4O_4$: C 66.97, H 5.15, N 13.02; found: C 67.18, H 5.22, N 13.09.

*6.1.5.6. Diethyl 2-[(4-hydroxyphenylamino) quinazolin-6-ylaminomethylene]-malonate (**6f**).* Yield 96%, mp 162–263.5 °C. IR: (ν_{max}, cm^{-1}): 3521, 3442 (2 NH), 3305 (OH), 2978 (aliphatic CH), 1642 (CO), 1641 (vinyl C=C) cm^{-1}. ^1H NMR (300 MHz) (DMSO-d_6) δ: 1.21–1.28 (2t, 6H, 2× –O–CH_2–CH_3), 4.18–4.25 (2q, 4H, 2× –O–CH_2–CH_3), 6.79–6.82 (d, 2H, anilino H_2, H_6), 7.42–7.48 (m, 2H, anilino H_3, H_5), 7.71–7.74 (d, 1H, quinazoline H_8, J = 9 Hz), 7.81–7.89 (dd, 1H, quinazoline H_7, J = 9 Hz, J = 1.8 Hz), 8.27–8.33 (d, 1H, quinazoline H_5, J = 1.8 Hz), 8.56 (s, 1H, quinazoline H_2), 8.57–8.61 (d, 1H, NH–CH=C, J = 13.5 Hz), 9.34 (s, 1H, phenolic–OH exchangeable by D_2O), 9.68 (s, 1H, anilino–NH exchangeable by D_2O), 10.97–11.01 (d, 1H, quinazoline NH, exchangeable by D_2O, J = 13.5 Hz). MS: m/z (%): 423 (M^+ + 1, 40%), 424 (M^+ + 2, 14.3%) & base peak at 376 (100%), Anal. Calcd. for $C_{22}H_{22}N_4O_5$: C 62.55, H 5.25, N 13.26; found: C 62.67, H 4.69, N 13.49.

6.1.6. General method for preparation of 4-(arylamino)-6-ureidoquinazoline (**7a**, **b**)

A mixture of appropriate amine (0.01 mol) and potassium cyanate (0.01 mol, 0.81 g) in glacial acetic acid was refluxed for about 2 h. After cooling; the crude product was filtered off, washed and crystallized from ethanol.

*6.1.6.1. 4-(4-Chlorophenylamino)-6-ureidoquinazoline (**7a**).* Yield 76%, mp 147–149 °C. IR: (ν_{max}, cm^{-1}): 3363 (NH's), 1686 (CO) cm^{-1}. ^1H NMR (300 MHz) (DMSO-d_6) δ: 6.11 (s, 2H, ureido–NH_2, exchangeable by D_2O), 7.45–7.49 (m, 2H, anilino H_2, H_6), 7.73–7.84 (m, 3H, quinazoline H_8 & anilino H_3, H_5), 7.89–7.92 (dd, 1H, quinazoline H_7, J = 9 Hz, J = 2.4 Hz), 8.46–8.47 (d, 1H, quinazoline H_5, J = 2.4 Hz), 8.46–8.57 (m, 1H, NH-CH=C), 8.60 (s, 1H, quinazoline H_2), 9.91 (s, 1H, anilino–NH, exchangeable by D_2O), 10.36 (s, 1H, quinazoline–NH, exchangeable by D_2O). ^{13}C NMR δ (ppm): 169.22, 158.30, 152.59, 143.91, 140.13, 138.34, 129.04, 128.88, 128.43, 127.69, 126.89, 124.89, 115.61, 112.32, 110.04, MS: m/z (%): 313.75 (M^+, 19.5%), 312.75 (M^+ − 1, 49.25%), 311.75 (M^+ − 2, 22.15%) & base peak at 51.7 (100%), Anal. Calcd. for $C_{15}H_{12}ClN_5O$: C 57.42, H 3.86, N 22.32; found: C 57.71, H 3.90, N 15.38.

*6.1.6.2. 4-(3-Hydroxyphenylamino)-6-ureidoquinazoline (**7b**).* Yield 86%, mp 271–272.5 °C. IR: (ν_{max}, cm^{-1}): 3423 (NH), 3313.11 (OH), 1701 (CO) cm^{-1}. ^1H NMR (300 MHz) (DMSO-d_6) δ: 6.16 (s, 2H, ureido–NH_2, exchangeable by D_2O), 6.49–6.53 (m, 1H, anilino H_2), 7.09–7.66 (m, 3H, anilino H_4, H_5, H_6), 7.70–7.73 (d, 1H, quinazoline H_8, J = 9 Hz), 7.89–7.93 (dd, 1H, quinazoline H_7, J = 9 Hz, J = 2.4 Hz), 8.46–8.47 (d, 1H, quinazoline H_5, J = 2.4 Hz), 8.668 (s, 1H, quinazoline H_2), 9.11 (s, 1H, OH, exchangeable by D_2O), 9.64 (s, 1H, anilino–NH, exchangeable by D_2O), 10.34 (s, 1H, quinazoline–NH exchangeable by D_2O). MS: m/z (%): 294 (M^+ − 1, 11.74%) & base peak at (108.85, 100%), Anal. Calcd. for $C_{15}H_{13}N_5O_2$: C 61.01, H 4.44, N 23.72; found: C 61.37, H 4.56, N 23.79.

6.2. Pharmacology

6.2.1. Materials and methods

6.2.1.1. In vitro EGFR tyrosine kinase activity. The EGFR tyrosine kinase activity at single dose concentration of 10 μM was carried out by BPS Bioscience (www.bpsbioscience.com) & EGFR (BPS#40187) served as the enzyme source and Poly (Glu, Tyr) sodium salt, (4:1, Glu:Tyr) (Sigma#P7244) served as the standardized substrate & Kinase-Glo Plus Luminescence kinase assay kit (Promega#V3772).

The IC_{50} determination was carried out where quality control testing is routinely performed on each of the targets to insure

compliance to acceptable standards. ^{33}P-ATP was purchased from Perkin Elmer and ADP-Glo™ was purchased from Promega. All other materials were of standard laboratory grade.

6.2.1.1.1. Assay protocols. The EGFR tyrosine kinase activity was performed using Kinase-Glo Plus luminescence kinase assay kit (Promega). It measures kinase activity by quantitating the amount of ATP remaining in solution following a kinase reaction. The luminescent signal from the assay is correlated with the amount of ATP present and is inversely correlated with the amount of kinase activity. The compounds were diluted to 100 μM in 10% DMSO and 5 μl of the dilution was added to a 50 μl reaction so that the final concentration of DMSO is 1% in all of reactions. All of the enzymatic reactions were conducted at 30 °C for 40 min. The 50 μl reaction mixture contains 40 mM Tris, pH 7.4, 10 mM $MgCl_2$, 0.1 mg/ml BSA, 0.2 mg/ml Poly (Glu, Tyr) substrate, 10 μM ATP and EGFR. After the enzymatic reaction, 50 μl of Kinase-Glo Plus Luminescence kinase assay solution (Promega) was added to each reaction and incubate the plate for 5 min at room temperature. Luminescence signal was measured using a Tecan Infinite M1000 microplate reader.

The protein kinase assays used to determine IC_{50} value were performed using ADP-GloTM assay kit from Promega which measures the generation of ADP by the protein kinase. Generation of ADP by the protein kinase reaction leads to an increase in luminescence signal in the presence of ADP-GloTM assay kit.

The assay was started by incubating the reaction mixture in a 96-well plate at 30 °C for 30 min. After the 30 min incubation period, the assay was terminated by the addition of 25 μl of ADP-GloTM Reagent (Promega). The 96-well plate was shaken and then incubated for 40 min at ambient temperature. 50 μl of Kinase detection reagent was added, the 96-well reaction plate was then read using the ADP-Glo Luminescences Protocol on a GloMax plate reader (Promega: Catalog #E7031). Blank control was set up that included all the assay components except the addition of appropriate substrate (replace with equal volume of kinase assay buffer). The corrected activity for each protein kinase target was determined by removing the blank control value.

6.2.1.1.2. Data analysis. EGFR activity assays were performed in duplicate at each concentration. The luminescence data were analyzed using the computer software, Graphpad Prism. The difference between luminescence intensities in the absence of EGFR (Lu_t) and in the presence of EGFR (Lu_c) was defined as 100% activity ($Lu_t - Lu_c$). Using luminescence signal (Lu) in the presence of the compound, % activity was calculated as:

% Activity = $\{(Lu_t - Lu)/(Lu_t - Lu_c)\} \times 100\%$, where Lu = the luminescence intensity in the presence of the compound (all percent activities below zero were set to 0%).

% Inhibition was calculated as: % inhibition = 100 (%) − % activity.

IC_{50} determination for inhibitor against EGFR was estimated by generating a graph of log inhibitor vs normalized response with variable using the Prism software.

6.2.1.2. Evaluation for cytotoxic activity against a panel of sixty human cancer cell lines. National Cancer Institute (NCI) for *in vitro* anticancer assay evaluates different compounds for their anticancer activity. The screening is a two-stage process, beginning with the evaluation of all compounds against the full NCI 60 cell lines panel representing leukemia, Non-Small Cell Lung Cancer, melanoma, colon cancer, CNS cancer, breast cancer, ovarian cancer, renal cancer and prostate cancer at a single dose of 10^{-5} M. The output from the single dose screen is reported as a mean graph and is available for analysis by the COMPARE program. Compounds which exhibit significant growth inhibition are evaluated against the 60 cell panel at five concentration levels.

a. Assay protocol

The human tumor cell lines of the cancer-screening panel are grown in RPMI 1640 medium containing 5% fetal bovine serum and 2 mM L-glutamine. For a typical screening experiment, cells are inoculated into 96 well microtiter plates in 100 ml at plating densities ranging from 5000 to 40,000 cells/well depending on the doubling time of individual cell lines. After cell inoculation, the microtiter plates are incubated at 37 °C, 5% CO_2, 95% air and 100% relative humidity for 24 h prior to addition of experimental drugs. After 24 h, two plates of each cell line are fixed in situ with TCA, to represent a measurement of the cell population for each cell line at the time of drug addition (Tz). Experimental drugs are solubilized in dimethyl sulfoxide at 400-fold the desired final maximum test concentration and stored frozen prior to use. At the time of drug addition, an aliquot of frozen concentrate is thawed and diluted to twice the desired final maximum test concentration with complete medium containing 50 mg/ml Gentamicin. Additional four, 10-fold or ½log serial dilutions are made to provide a total of five drug concentrations plus control. Aliquots of 100 ml of these different drug dilutions are added to the appropriate microtiter wells already containing 100 ml of medium, resulting in the required final drug concentrations. Following drug addition, the plates are incubated for an additional 48 h at 37 °C, 5% CO_2, 95% air, and 100% relative humidity. For adherent cells, the assay is terminated by the addition of cold TCA. Cells are fixed in situ by the gentle addition of 50 ml of cold 50% (w/v) TCA (final concentration, 10% TCA) and incubated for 60 min at 4 °C. The supernatant is discarded, and the plates are washed five times with tap water and air dried. Sulforhodamine B (SRB) solution (100 ml) at 0.4% (w/v) in 1% acetic acid is added to each well, and plates are incubated for 10 min at room temperature. After staining, unbound dye is removed by washing five times with 1% acetic acid and the plates are air dried. Bound stain is subsequently solubilized with 10 mM trizma base, and the absorbance is read on an automated plate reader at a wavelength of 515 nm. For suspension cells, the methodology is the same except that the assay is terminated by fixing settled cells at the bottom of the wells by gently adding 50 ml of 80% TCA (final concentration, 16% TCA)

b. Data analysis

Using the seven absorbance measurements [time zero, (Tz), control growth, (C), and test growth in the presence of drug at the five concentration levels (Ti)], the percentage growth is calculated at each of the drug concentrations levels. Percentage growth inhibition is calculated as: $[(Ti - Tz)/(C - Tz)] \times 100$ for concentrations for which $Ti >/ = Tz$ and $[(Ti - Tz)/Tz] \times 100$ for concentrations for which $Ti < Tz$: three dose response parameters are calculated for each experimental agent. Growth inhibition of 50% (GI_{50}) is calculated from $[(Ti - Tz)/(C - Tz)] \times 100 = 50$, which is the drug concentration resulting in a 50% reduction in the net protein increase (as measured by SRB staining) in control cells during the drug incubation. The drug concentration resulting in total growth inhibition (TGI) is calculated from Ti ¼ Tz. The LC_{50} (concentration of drug resulting in a 50% reduction in the measured protein at the end of the drug treatment as compared to that at the beginning) indicating a net loss of cells following treatment is calculated from $[(Ti - Tz)/Tz] \times 100 = -50$. Values are calculated for each of these three parameters if the level of activity is reached; however, if the effect is not reached or is exceeded, the value for that parameter is expressed as greater or less than the maximum or minimum concentration tested [41,42].

Results for each compound were reported as a mean graph of the percent growth of the treated cells when compared to the untreated control cells. There after obtaining the results for one

dose assay, analysis of historical Development Therapeutics Programme (DTP) was performed and compounds which satisfies predetermined threshold inhibition criteria is selected for NCI full panel 5 dose assay.

6.3. Docking studies

All molecular modeling calculation and docking studies were carried out using GOLD 4.1 [26]. The X-ray crystal structure of the kinase domain of EGFR in complex with its inhibitor (PDB code 2J5F) was recovered RSCB protein data bank, which was chosen because of the interaction between the 6-substitution of the inhibitor to unique Cys-793 of EGFR. Docking engine was validated; the co-crystallized ligand was extracted from the catalytic site and redocked to calculate the root mean square difference (RMSD) between the top docking pose and original crystallographic geometry. The protein structure was prepared using protein preparation protocol of Accelry's discovery studio 2.5 [43]. The amino acid residues were ionized using role based technique and the missing residues were completed. The protein structure was typed by CHARMM [44] force field then it was minimized using 500 step of SMART minimizer of Discovery studio program (Minimizer adopt hybrid of steepest descent [45] and conjugate gradient [46] minimization algorithms). All the water molecules in the protein were deleted except No. 10 because of its main role in ligand binding. Based on the literature data of EGFR-TK inhibitors binding [14,15], an interaction motif was added to Met-769 residue as hydrogen bond donor. Kinase template was loaded in gold and the default parameters of GOLD were used except that the number of operations was raised to 500,000 operations and the selection pressure rose to 1.1. Chemscore kinase scoring function was used to score the resulted docking poses [47].

Acknowledgments

The authors are grateful to The National Cancer Institute, Maryland, USA for performing anticancer activity and also would like also to thank BPS Bioscience for EGFR binding assay.

Appendix A. Supplementary data

Supplementary data related to this article can be found at http://dx.doi.org/10.1016/j.ejmech.2012.10.017.

References

[1] M.A. Olayioye, R.M. Neve, H.A. Lane, N.E. Hynes, The ErbB signaling network: receptor heterodimerization in development and cancer, EMBO J. 19 (2000) 3159–3167.
[2] W. Alan, EGF receptor, Int. J. Biochem. Cell. Biol. 31 (1999) 637–643.
[3] H.-Q. Li, D.-D. Li, X. Lu, Y.-Y. Xu, H.-L. Zhu, Design and synthesis of 4,6-substituted-(diaphenylamino)quinazolines as potent EGFR inhibitors with antitumor activity, Bioorg. Med. Chem. 20 (2012) 317–323.
[4] W.J. Gullick, Prevalence of aberrant expression of the epidermal growth factor receptor in human cancers, Br. Med. Bull. 47 (1991) 87–98.
[5] C.J. Wikstrand, R.E. McLendon, A.H. Friedman, D.D. Bigner, Cell surface localization and density of the tumor-associated variant of the epidermal growth factor receptor, EGFRvIII, Cancer Res. 57 (1997) 4130–4140.
[6] W.K. Hong, A. Ullrich, The role of EGFR in solid tumors and implications for therapy, Oncol. Biother. 1 (2000) 1–29.
[7] E. Zwick, J. Bange, A. Ullrich, Receptor tyrosine kinase signalling as a target for cancer intervention strategies, Endocr. Relat. Cancer 8 (2001) 161–173.
[8] C. Fernandes, C. Oliveira, L. Gano, A. Bourkoula, I. Pirmettis, I. Santos, Radioiodination of new EGFR inhibitors as potential SPECT agents for molecular imaging of breast cancer, Bioorg. Med. Chem. 15 (2007) 3974–3980.
[9] L.T. Liu, T.-T. Yuan, H.-H. Liu, S.-F. Chen, Y.-T. Wu, Synthesis and biological evaluation of substituted 6-alkynyl-4-anilinoquinazoline derivatives as potent EGFR inhibitors, Bioorg. Med. Chem. Lett. 17 (2007) 6373–6377.
[10] J.C. Delarue, P. Terrier, M.J. Terrier-Lacombe, H. Mouriesse, M. Gotteland, F. May-Levin, Combined overexpression of c-erbB-2 protein and epidermal growth factor receptor (EGF-R) could be predictive of early and long-term outcome in human breast cancer: a pilot study, Bull. Cancer 81 (1994) 1067–1077.
[11] S.M. Abou-Seri, Synthesis and biological evaluation of novel 2,4′-bis substituted diphenylamines as anticancer agents and potential epidermal growth factor receptor tyrosine kinase inhibitors, Eur. J. Med. Chem. 45 (2010) 4113–4121.
[12] A. Antonello, A. Tarozzi, F. Morroni, A. Cavalli, M. Rosini, P. Hrelia, M.L. Bolognesi, C. Melchiorre, Multitarget-directed drug design strategy: a novel molecule designed to block epidermal growth factor receptor (EGFR) and to exert proapoptotic effects†, J. Med. Chem. 49 (2006) 6642–6645.
[13] B.C. Roger, Epidermal growth factor receptor as a therapeutic target in colorectal cancer, Clin. Colorectal Cancer 2 (2003) 246–251.
[14] J.J.-L. Liao, Molecular recognition of protein kinase binding pockets for design of potent and selective kinase inhibitors, J. Med. Chem. 50 (2007) 409–424.
[15] J. Stamos, M.X. Sliwkowski, C. Eigenbrot, Structure of the epidermal growth factor receptor kinase domain alone and in complex with a 4-anilinoquinazoline inhibitor, J. Biol. Chem. 277 (2002) 46265–46272.
[16] R.-D. Li, X. Zhang, Q.-Y. Li, Z.-M. Ge, R.-T. Li, Novel EGFR inhibitors prepared by combination of dithiocarbamic acid esters and 4-anilinoquinazolines, Bioorg. Med. Chem. Lett. 21 (2011) 3637–3640.
[17] P. Ballard, R.H. Bradbury, C.S. Harris, L.F.A. Hennequin, M. Hickinson, P.D. Johnson, J.G. Kettle, T. Klinowska, A.G. Leach, R. Morgentin, M. Pass, D.J. Ogilvie, A. Olivier, N. Warin, E.J. Williams, Inhibitors of epidermal growth factor receptor tyrosine kinase: novel C-5 substituted anilinoquinazolines designed to target the ribose pocket, Bioorg. Med. Chem. Lett. 16 (2006) 1633–1637.
[18] V.G. Pawar, M.L. Sos, H.B. Rode, M. Rabiller, S. Heynck, W.A.L. van Otterlo, R.K. Thomas, D. Rauh, Synthesis and biological evaluation of 4-anilinoquinolines as potent inhibitors of epidermal growth factor receptor, J. Med. Chem. 53 (2010) 2892–2901.
[19] J.B. Smaill, G.W. Rewcastle, J.A. Loo, K.D. Greis, O.H. Chan, E.L. Reyner, E. Lipka, H.D.H. Showalter, P.W. Vincent, W.L. Elliott, W.A. Denny, Tyrosine kinase inhibitors. 17. Irreversible inhibitors of the epidermal growth factor receptor: 4-(phenylamino)quinazoline- and 4-(phenylamino)pyrido[3,2-d]pyrimidine-6-acrylamides bearing additional solubilizing functions, J. Med. Chem. 43 (2000) 1380–1397.
[20] W.A. Denny, Irreversible inhibitors of the erbB family of protein tyrosine kinases, Pharmacol. Ther. 93 (2002) 253–261.
[21] J.B. Smaill, B.D. Palmer, G.W. Rewcastle, W.A. Denny, D.J. McNamara, E.M. Dobrusin, A.J. Bridges, H. Zhou, H.D.H. Showalter, R.T. Winters, W.R. Leopold, D.W. Fry, J.M. Nelson, V. Slintak, W.L. Elliot, B.J. Roberts, P.W. Vincent, S.J. Patmore, Tyrosine kinase inhibitors. 15. 4-(phenylamino)quinazoline and 4-(phenylamino)pyrido[d]pyrimidine acrylamides as irreversible inhibitors of the ATP binding site of the epidermal growth factor receptor, J. Med. Chem. 42 (1999) 1803–1815.
[22] D.W. Fry, A.J. Bridges, W.A. Denny, A. Doherty, K.D. Greis, J.L. Hicks, K.E. Hook, P.R. Keller, W.R. Leopold, J.A. Loo, D.J. McNamara, J.M. Nelson, V. Sherwood, J.B. Smaill, S. Trumpp-Kallmeyer, E.M. Dobrusin, Specific, irreversible inactivation of the epidermal growth factor receptor and erbB2, by a new class of tyrosine kinase inhibitor, Proc. Natl. Acad. Sci. U. S. A. 95 (1998) 12022–12027.
[23] A. Wissner, D.M. Berger, D.H. Boschelli, M.B. Floyd, L.M. Greenberger, B.C. Gruber, B.D. Johnson, N. Mamuya, R. Nilakantan, M.F. Reich, R. Shen, H.-R. Tsou, E. Upeslacis, Y.F. Wang, B. Wu, F. Ye, N. Zhang, 4-Anilino-6,7-dialkoxyquinoline-3-carbonitrile inhibitors of epidermal growth factor receptor kinase and their bioisosteric relationship to the 4-anilino-6,7-dialkoxyquinazoline inhibitors, J. Med. Chem. 43 (2000) 3244–3256.
[24] J.B. Smaill, H.D.H. Showalter, H. Zhou, A.J. Bridges, D.J. McNamara, D.W. Fry, J.M. Nelson, V. Sherwood, P.W. Vincent, B.J. Roberts, W.L. Elliott, W.A. Denny, Tyrosine kinase inhibitors. 18. 6-substituted 4-anilinoquinazolines and 4-anilinopyrido[3,4-d]pyrimidines as soluble, irreversible inhibitors of the epidermal growth factor receptor, J. Med. Chem. 44 (2000) 429–440.
[25] G.W. Rewcastle, W.A. Denny, A.J. Bridges, H. Zhou, D.R. Cody, A. McMichael, D.W. Fry, Tyrosine kinase inhibitors. 5. Synthesis and structure-activity relationships for 4-[(phenylmethyl)amino]- and 4-(phenylamino)quinazolines as potent adenosine 5'-triphosphate binding site inhibitors of the tyrosine kinase domain of the epidermal growth factor receptor, J. Med. Chem. 38 (1995) 3482–3487.
[26] GOLD 4.1. www.ccdc.cam.ac.uk.
[27] H.-R. Tsou, N. Mamuya, B.D. Johnson, M.F. Reich, B.C. Gruber, F. Ye, R. Nilakantan, R. Shen, C. Discafani, R. DeBlanc, R. Davis, F.E. Koehn, L.M. Greenberger, Y.-F. Wang, A. Wissner, 6-Substituted-4-(3-bromophenylamino)quinazolines as putative irreversible inhibitors of the epidermal growth factor receptor (EGFR) and human epidermal growth factor receptor (HER-2) tyrosine kinases with enhanced antitumor activity, J. Med. Chem. 44 (2001) 2719–2734.
[28] R. Albuschat, W. Löwe, M. Weber, P. Luger, V. Jendrossek, 4-Anilinoquinazolines with lavendustin A subunit as inhibitors of epidermal growth factor receptor tyrosine kinase: syntheses, chemical and pharmacological properties, Eur. J. Med. Chem. 39 (2004) 1001–1011.
[29] B. Marvania, P.-C. Lee, R. Chaniyara, H. Dong, S. Suman, R. Kakadiya, T.-C. Chou, T.-C. Lee, A. Shah, T.-L. Su, Design, synthesis and antitumor evaluation of phenyl N-mustard-quinazoline conjugates, Bioorg. Med. Chem. 19 (2011) 1987–1998.
[30] E. Knippel, M. Knippel, M. Michalik, H. Kelling, H. Kristen, On the geometric isomers of ethyl 2-nitro-3-ethoxyacrylate, ethyl 2-nitro-3-phenylaminoacrylate and ethyl 2-cyano-3-phenylaminoacrylate, Tetrahedron 33 (1977) 231–234.

[31] W. Bottomley, J.N. Phillips, J.G. Wilson, H–N–C–H coupling in the NMR spectra of 3-aminoacrylic esters, Tetrahedron Lett. 8 (1967) 2957–2961.
[32] A.E. Wakeling, A.J. Barker, D.H. Davies, D.S. Brown, L.R. Green, S.A. Cartlidge, J.R. Woodburn, Specific inhibition of epidermal growth factor receptor tyrosine kinase by 4-anilinoquinazolines, Breast Cancer Res. Treat. 38 (1996) 67–73.
[33] K. Wosikowski, D. Schuurhuis, K. Johnson, S.E. Bates, K.D. Paull, T.G. Myers, J.N. Weinstein, Identification of epidermal growth factor receptor and c-erbB2 pathway inhibitors by correlation with gene expression patterns, J. Natl. Cancer Inst. 89 (1997) 1505–1515.
[34] R.H. Shoemaker, The NCI60 human tumour cell line anticancer drug screen, Nat. Rev. Cancer 6 (2006) 813–823.
[35] X. Wu, M. Li, Y. Qu, W. Tang, Y. Zheng, J. Lian, M. Ji, L. Xu, Design and synthesis of novel gefitinib analogues with improved anti-tumor activity, Bioorg. Med. Chem. 18 (2010) 3812–3822.
[36] G. Jones, P. Willett, R.C. Glen, A.R. Leach, R. Taylor, Development and validation of a genetic algorithm for flexible docking, J. Mol. Biol. 267 (1997) 727–748.
[37] C.-H. Yun, T.J. Boggon, Y. Li, M.S. Woo, H. Greulich, M. Meyerson, M.J. Eck, Structures of lung cancer-derived EGFr mutants and inhibitor complexes: mechanism of activation and insights into differential inhibitor sensitivity, Cancer Cell 11 (2007) 217–227.
[38] S. Madapa, Z. Tusi, A. Mishra, K. Srivastava, S.K. Pandey, R. Tripathi, S.K. Puri, S. Batra, Search for new pharmacophores for antimalarial activity. Part II: synthesis and antimalarial activity of new 6-ureido-4-anilinoquinazolines, Bioorg. Med. Chem. 17 (2009) 222–234.
[39] S. Botros, K.M. Ghoneim, M. Khalifa, synthesis of certain nitroquinazoline-dervatives structurally related to some chemotherapeutic agents, Egypt. J. Pharm. Sci. 13 (1972) 11–21.
[40] H.A.A. Shady, S.L. El-Ansary, D.A.A. El-Ella, N.A. Farag, Benzopyranone derivatives (Part 1): synthesis of various benzopyranoylimidazolidinetriones, arylpyranobenzoxazinone, pyranobenzoxazinetrione and benzopyranoyl-triazinetrione derivatives of potential CNS depresant activity, Bull. Fac. Pharm. Cairo Univ. 42 (2004) 31–42.
[41] M.C. Alley, D.A. Scudiero, A. Monks, M.L. Hursey, M.J. Czerwinski, D.L. Fine, B.J. Abbott, J.G. Mayo, R.H. Shoemaker, M.R. Boyd, Feasibility of drug screening with panels of human tumor cell lines using a microculture tetrazolium assay, Cancer Res. 48 (1988) 589–601.
[42] M.R. Grever, S.A. Schepartz, B.A. Chabner, The National Cancer Institute: cancer drug discovery and development program, Semin. Oncol. 19 (1992) 622–638.
[43] Accelry's Discovery Studio 2.5.5, Accelrys Software Inc., San Diego, 2010.
[44] B.R. Brooks, R.E. Bruccoleri, B.D. Olafson, D.J. States, S. Swaminathan, M. Karplus, CHARMM: a program for macromolecular energy, minimization, and dynamics calculations, J. Comp. Chem. 4 (1983) 187–217.
[45] P. Debye, Näherungsformeln für die Zylinderfunktionen für große Werte des Arguments und unbeschränkt veränderliche Werte des Index, Mathematische Annalen 67 (1909) 535–558.
[46] R. Fletcher, C.M. Reeves, Function minimization by conjugate gradients, Comput. J. 7 (1964) 149–154.
[47] K. Choowongkomon, O. Sawatdichaikul, N. Songtawee, J. Limtrakul, Receptor-based virtual screening of EGFR kinase inhibitors from the NCI diversity database, Molecules 15 (2010) 4041–4054.